EVALUATION OF STATIC STABILITY DERIVATIVES FROM STANDARD YAWING TESTS

by

Richard Noble de Callies

A Thesis Submitted in Partial Fulfillment
of the Requirements for the Degree of
Master of Science

STEVENS INSTITUTE OF TECHNOLOGY
Hoboken New Jersey

EVALUATION OF STATIC STABILITY DERIVATIVES FROM STANDARD YAWING TESTS

A Thesis Submitted in Partial Fulfillment
of the Requirements for the Degree of
Master of Science

STEVENS INSTITUTE OF TECHNOLOGY

Submitted by Richard Noble de Callies

TABLE OF CONTENTS

SUMMARY

An analytical and experimental investigation was made to determine the possibility of predicting the static and rotary directional stability derivatives of a flying boat of the conventional short-afterbody type. Starting with the angle of trim obtained from a tank test at a specified load and speed, the extent of the wetted areas of forebody and afterbody is computed on the basis of available empirical relations available for planing processes. It is shown that for a range of pre-hump speed the lateral forces due to the yaw can be obtained by consideration of the inequality of loading on two sides of the bottom due to the change of the effective angles of attack resulting from vectorial addition of the angles of deadrise, yaw, and trim. It is also shown that this action results in identical position of centers of pressure for the vertical and lateral forces. On this basis, the static and rotary stability derivatives for yawing motion are computed.

The experimental verification of the method in regards to static derivatives was made for three operating speeds at C_V of 2.63, 2.46, and 2.34. A reasonable agreement of the test and analysis data is shown for the two higher speeds, but the agreement at the lowest speed is uncertain, probably because of the lack of necessary data on the configuration of the wake of the forebody. Such data are presently available only for C_V of 3.0 and above.

The work was done at the Graduate School and Experimental Towing Tank of Stevens Institute of Technology in partial fulfillment of the requirements for the degree of Master of Science.

INTRODUCTION

Locke and Pierson (References 1 and 2) among others point to the ever-increasing instances of flying-boat directional instability in the past years with an increase in operating loads, especially in the pre-hump region. Many investigations on specific types of hulls have been carried out in order to determine what kind of modifications to the hull will give the best directional stability. Extended afterbody and planing-tail hulls (Reference 3) have received quite a bit of attention. Besides considering the type of hull which will best give the desired directional stability, much of the present work has been directed toward auxiliary devices which will aid directional control in the pre-hump region. Such devices include water-rudders (Reference 4), reversible-pitch propellers and hydro-flaps (Reference 5). Hydro-flaps appear as an excellent means of obtaining good directional control. From current trends it is entirely possible that the problem of directional control in the pre-hump region will be neatly by-passed in favor of auxiliary control devices and little attention will be paid to the basic hull unless the hull should exhibit some extremely radical directional tendencies.

It is the intent of the present work to return to the basic hull without any auxiliary control devices and to determine what the hull stability will be from data obtained in ordinary planing test runs. The inherent directional instability of the forebody is due to the excessive wetted length extending forward

of the C.G. of the forebody (Reference 6). Therefore the afterbody must supply the necessary stabilizing moment for the entire hull to be directionally stable. The contribution to stability of the afterbody is extremely difficult to predict because of the changes in the wave form in the wake brought about by changes in trim and speed of the forebody. The yawing moments due to the afterbody directly depend, of course, on this shape of the wake. The moments created by the afterbody can be considered to be of two types. The first is due to the shape of the afterbody and the shape of the wake while the second is of an accidental nature. That is, moments of the second type are due to water flowing over the curved sides of the afterbody or over various portions of the tail cone. Attention is concentrated only on the first type since the second type is not amenable to any simple analysis, being dealt with in practice by the use of stringers and other type of flow-corrective devices.

There is quite a bit of available information on porpoising and longitudinal stability, but very little information concerning directional stability, especially from an analytical viewpoint. This is due to the complex nature of the flow existing around the afterbody as already suggested. In the early stages of the present investigation, it was felt that the range of investigation should be limited to the pre-hump region where most of the instability of the seaplanes is encountered. In the region between hump and getaway, the hull has either sufficient inherent directional stability or aerodynamic and thrust control sufficient to maintain a straight course. The range of investi-

gation was also limited to the horizontal plane. That is, heel angle, rolling, and pitching velocities were neglected.

The general problem of the pre-hump region involves both low-speed taxiing as well as pre-hump speeds involved during take-off. This report as well as being limited to the pre-hump region also excludes low-speed taxiing. This choice has been made since during pre-hump speeds used for take-off, the sides are essentially dry and most of the weight is supported by dynamic loads on the forebody and afterbody and therefore use can be made of available planing theory. In the case of low-speed taxiing, it is not possible to use the simpler planing theory, since the curved portion of the forebody and sides are wet. Any analysis for low-speed taxiing is complicated and involved.

Using a composite chart of directional stability for a conventional short-afterbody hull of well-known design (Reference 1), three speed coefficients (2.34, 2.46, and 2.63) were chosen for which the directional stability derivatives were to be predicted. The static directional stability derivatives in nondimensional form were available for only one of the speeds chosen from Reference 7. Moment due to yaw and transverse force due to zero angle of yaw (i.e., on-course motion) were reported in this case for the speed coefficient of 2.62. The fundamental problem is to find a mathematical analysis which predicts the existence of certain forces on the hull, and to show that by the existence of these forces the static stability already known must result.

For the speed coefficient of 2.62, the analysis will proceed on the following basis. The centers of pressure of both the forebody and the afterbody will be determined. The assumption is then made that for small deviations from a straight course the centers of pressure and the wetted lengths of both the forebody and the afterbody do not change but remain fixed. Since the problem has already been confined to speed ranges where the sides are not wetted, and therefore since only the bottom areas are wetted, it may be concluded that the lateral force produced due to an inequality of pressures on the two sides of the hull acts at the same point as the vertical force produced by planing action. That is, the centers of pressure for lateral loads and for vertical loads are coincident. For the case of zero yaw angle, the pressures acting on either side of a vee-bottom hull have a vertical and horizontal component of which the horizontal forces, being equal and opposite, cancel each other.

When the hull is given some arbitrary small yaw angle, a change in the effective angle of trim results which is positive for one side of the hull and negative for the other. Therefore the lifting force will be increased on one side of the hull bottom and decreased on the other. The horizontal components of these changing lift forces are opposite but no longer equal, and a resultant horizontal force will be produced. This type of analysis is also applicable to the afterbody but with the additional consideration of the change of the water surface in the wake.

As the hull is placed at some angle of yaw, the afterbody is displaced and the wake is no longer symmetrical about it. The mean lateral inclination of the water surface in the wake will cause the additional inclination of the resultant force, thereby producing an additional lateral force.

The sum of the horizontal forces on the forebody and afterbody will indicate the magnitude of transverse force produced by a given yaw angle. The horizontal forces multiplied by their respective arms, as determined from the centers of pressure of the vertical planing forces produced, will give the magnitude of the yawing moment produced for the same given yaw angle. It will be shown that satisfactory agreement with known static stability derivatives will be obtained by this method.

The distances from the centers of pressure of the forebody and afterbody having been determined, certain relations may be formalized which make use of these distances and the static stability derivatives, in order to obtain the rotary derivatives. In this connection, use is made of practices common in the solution of aircraft dynamic stability. An angular velocity creates a small change in the local yaw angle of the forebody and afterbody which will in turn produce additional transverse forces. The transverse velocities produced by the angular velocity will be proportional to the distance the force is located from the center of gravity. The change in yaw angle at each center of pressure will then be a function of the ratio of the local trans-

verse velocity and the incoming velocity. By following these principles, the expressions for the rotary derivatives using static stability derivatives may be derived as shown in the section on mathematical development.

Once all the derivatives have been established, the complete dynamic stability can be determined by resorting to the solution of the equations of motion as developed in Appendix I. The dynamic stability will be seen to depend on static transverse forces, static yawing moments, rotary transverse forces, rotary yawing moments, and the hull inertia parameters. The derivation in Appendix I is presented only in the interest of the complete picture of hull stability and no attempt is made for a solution of the roots. Suffice to say that positive roots indicate amplification of the disturbance while negative roots indicate a decay of the disturbance leading to stability (Reference 8).

Static stability has been defined as the tendency of a disturbance to disappear with time with the center of gravity constrained to move in a straight line. Therefore, the tests conducted in this investigation produce a measure of static stability since the C.G. is constrained. Under such conditions, four types of moment vs. yaw curves may result (Reference 9):

Type of Stability	Slope of $\partial N'/\partial \beta$
positive stability	negative
neutral	very small positive or zero
negative stability	positive
"hooking" instability	curve discontinuous at small angles

Of the types of moment curves possible, the statically stable type were obtained for the three cases tested in this investigation. However, the lowest speed coefficient used came quite close to the beginning of the region of "hooking" instability. It is not considered unfortunate that three cases were chosen in which the hull used was known to be stable. The primary intention of this investigation is to illustrate that the analytical method presented has application in the range chosen.

It has been suggested in other reports (Reference 7) that static stability is not a good criterion of dynamic stability. In fact, several instances of static instability in model testing have been shown by calculation to be dynamically stable. Criticism against static stability suggests that it is an artificial concept and in effect presupposes a lateral constraint which is not present and artificially removes from the free body one degree of freedom. In the present work, only the directional stability is considered, but the reader is reminded that the rotary derivatives are also necessary if the maneuvering characteristics are to be investigated.

The tank tests in this investigation were conducted in Tank No. 1 of the Experimental Towing Tank, Stevens Institute of Technology, Hoboken, New Jersey.

Acknowledgement is made to the personnel of the Experimental Towing Tank who helped in many ways with the work at all stages. Particular gratitude is due Professor B.V. Korvin-Kroukovsky for his very valuable help and patient advice.

SYMBOLS

Nondimensional Coefficients

C_Δ	Load coefficient	$C_\Delta = \Delta/wb^3$
C_V	Speed coefficient	$C_V = V/\sqrt{gb}$
C_M	Hydrodynamic trimming moment coefficient	$C_M = M/wb^4$
N'	Hydrodynamic yawing moment coefficient	$N' = N/\frac{\rho}{2}V^2b^3$
Y'	Hydrodynamic transverse force coefficient	$Y' = Y/\frac{\rho}{2}V^2b^2$
r'	Dimensionless angular velocity about Z-axis	$r' = rb/V$
C_r	Resistance coefficient	$C_r = R/\frac{\rho}{2}V^2b^2$
F_1'	Dimensionless hydrodynamic force coefficient at C.P. of forebody	$F_1' = F_1/\frac{\rho}{2}V^2b^2$
F_2'	Dimensionless hydrodynamic force coefficient at C.P. of afterbody	$F_2' = F_2/\frac{\rho}{2}V^2b^2$
C_{L_β}	Coefficient of lift (vee planing surface)	$C_{L_\beta} = 2C_\Delta/C_V^2$
C_{L_o}	Coefficient of lift (flat planing surface)	
C_F	Coefficient of friction drag	
λ	Ratio of mean wetted length to maximum beam	
Re	Reynolds number	

Forces and Moments

N	Hydrodynamic yawing moment about Z-axis (moments positive as per right-hand rule)
Y	Hydrodynamic force along Y-axis (force positive to starboard)
R	Hull resistance
F_1	Hydrodynamic transverse force at C.P. of forebody
F_2	Hydrodynamic transverse force at C.P. of afterbody

Derivatives

N'_β	Static hydrodynamic yawing moment coefficient derivative	$N'_\beta = \partial N'/\partial \beta$
Y'_β	Static hydrodynamic transverse force coefficient derivative	$Y'_\beta = \partial Y'/\partial \beta$
N'_r	Rotary hydrodynamic yawing moment coefficient derivative	$N'_r = \partial N'/\partial r'$
Y'_r	Rotary hydrodynamic transverse force coefficient derivative	$Y'_r = \partial Y'/\partial r'$

Other Symbols

b	Maximum beam, ft.
V	Velocity, ft./sec.
β	Yaw angle, deg.; angle between the velocity vector at C.G. and the X-axis (yaws positive about Z-axis in accordance with right-hand rule)
τ	Trim angle, deg.; angle between the undisturbed water level and the keel reference line (trim positive when keel line makes bow end above undisturbed water level)
Δ	Displacement weight, lb.
ℓ	Distance from C.G. to center of pressure; subscript 1 for forebody, subscript 2 for afterbody
ℓ_m	Mean wetted length
ℓ_c	Chine wetted length
ℓ_k	Keel wetted length
m	Subscript for all data applying to model

Constants

g	Acceleration of gravity (32.2 ft./sec.^{2})
w	Specific weight of water (62.3 lb./ft.^{3})
ρ	Density of water (1.937 slugs/ft.^{3})
ν	Kinematic viscosity of fresh water (1.08×10^{-5} ft.^{2}/sec. at 20° centigrade)

ANALYTICAL DEVELOPMENT AND MATHEMATICAL ANALYSIS

The forces acting on a hull in two-step planing due to some given angle of yaw may be represented as shown in Figure 1(a). That is, at some angle of yaw there will be a moment about the C.G. and a transverse force which may be imagined to act at the C.G.

The transverse forces and moments produced by varying the angle of yaw represent the static stability derivatives $\partial N'/\partial \beta$ and $\partial Y'/\partial \beta$. Actually, the true picture of the situation is presented in Figure 1(b), where the transverse force is seen to be the addition of two transverse forces, one acting at the forebody center of pressure and the other at the afterbody center of pressure. The moment about the C.G. is the result of the forebody and afterbody forces acting at their respective arms. Yaw angle, hydrodynamic yawing moment and transverse forces are all assumed to be positive. Using the notation shown, the two fundamental relations will be:

$$Y = F_1 + F_2 \qquad (1)$$

$$N = F_1 \ell_1 - F_2 \ell_2 \qquad (2)$$

Solving these equations, an expression for the forces F_1 and F_2 may be derived as follows:

Eliminating F_1 in equations (1) and (2) gives:

$$N = \ell_1 (Y - F_2) - F_2 \ell_2$$

$$N = - F_2 (\ell_1 + \ell_2) + \ell_1 Y .$$

Therefore,

$$F_2 = \frac{\ell_1 Y - N}{\ell_1 + \ell_2} \quad . \tag{3}$$

Substituting the value of F_2 in equation (1) gives

$$F_1 = Y - \frac{\ell_1 Y - N}{\ell_1 + \ell_2} \quad .$$

Therefore,

$$F_1 = \frac{N + \ell_2 Y}{\ell_1 + \ell_2} \quad .$$

Forebody Planing Data

Having obtained expressions for the forces F_1 and F_2, it is necessary to determine the centers of pressure of the forebody and afterbody. Leaving the equations for F_1 and F_2, previous data are analyzed for hull conditions which led to known values of the static derivatives. Table I gives the necessary model dimensions while Condition 1 in Table IV gives the basic knownquantities for the hull to be analyzed.

It was necessary to begin with an assumption concerning the amount of the total load carried by the forebody alone, since the load coefficient for Condition 1 was that for the entire hull. Once the assumption has been made, the hull analyzed, and all conditions found to be in agreement, the assumption is no longer an assumption but becomes a fact leading to a unique solution. In view of the relative loads in two-step planing above the hump, it seemed reasonable to assume that under present conditions the forebody carried 81% of the total load. Therefore $C_\Delta = .81(.8) = .648$. From the equation of lift coefficient due

to an angle of deadrise,

$$C_{L_\beta} = \frac{2C_\Delta}{C_V^2} = \frac{2(.648)}{6.87} = .1885 \quad . \tag{5}$$

Unfortunately, the relations involving lift coefficient and the aspect ratio of the wetted area are such which require trial and error solution if recourse is not made to nomographs available in Reference 6. It was found that the equations gave more satisfactory results because of the greater accuracy. By trial and error, then, the value of the lift coefficient for a zero deadrise planing surface is obtained from the lift coefficient of a vee-planing surface:

$$C_{L_\beta} = C_{L_o} - .0065(\beta)\, C_{L_o}^{.6} \tag{6}$$

$$\begin{aligned} C_{L_\beta} &= C_{L_o} - .143\, C_{L_o}^{.6} \\ &= .251 - .143\,(.436) \\ &= .251 - .0623 \\ &= .1887 \quad . \end{aligned}$$

Therefore,

$$C_{L_o} = .251 \quad .$$

To determine the aspect ratio, the following relation is used:

$$\frac{C_{L_o}}{C^{1.1}} = .0120(\lambda)^{\frac{1}{2}} + .0095\,\frac{\lambda^2}{C_V^2} \quad , \tag{7}$$

which, for the values required, reduces to

$$.0155 = .0120(\lambda)^{\frac{1}{2}} + .00138(\lambda)^2 \quad .$$

Once again by trial and error, the following is obtained:

$$\frac{C_{L_o}}{\tau^{1.1}} = .0120(1.25)^{\frac{1}{2}} + .00138(1.25)^2$$

$$= .0134 + .00215$$

$$= .01555 \quad .$$

Therefore, the aspect ratio becomes

$$\lambda = 1.25 \quad .$$

Savitsky (Reference 10) has presented the following formulation for determining the position of the center of pressure of a vee-planing surface:

$$C_P = .75 - \frac{1}{3.06 \frac{C_V^2}{\lambda^{3/2}} + 2.42} \qquad (8)$$

where

$$C_P = \frac{P}{\ell_m} \quad ,$$

P being the distance on the forebody from the step.

For the forebody being considered here, results indicate that

$$C_P = .75 - \frac{1}{3.06 \frac{(2.62)^2}{(1.25)^{3/2}} + 2.42}$$

$$= .75 - \frac{1}{15.05 + 2.42}$$

$$= .75 - .057 \quad .$$

Therefore

$$C_P = .693 \quad .$$

By definition,

$$\lambda = \frac{\ell_m}{b} \quad , \tag{9}$$

and therefore,

$$\ell_m = 10(1.25) = 12.5 \text{ ft.}$$

That is, the mean wetted length of the forebody is 12.5 ft. And from the definition of the center of pressure coefficient,

$$\ell_P = .693(12.5) = 8.66 \text{ ft.}$$

The point of center of pressure of the forebody is 8.66 ft. forward of the step. However, the dimension desired is ℓ_1 which is defined as the distance of the center of pressure from the C.G. For this investigation, the C.G. was considered to be 3.67 ft. forward of the step. Therefore

$$\ell_1 = 8.66 - 3.67$$

$$\ell_1 = 4.99 \text{ ft.}$$

Longitudinal Wave Profile

In order to determine the hydrodynamic force on the afterbody, it is necessary to plot the afterbody to scale, determine the longitudinal wave profile, and from this determine the angle of trim of the afterbody and the beam. This is a critical calculation since the load computed by reference to the longitudinal wave profile must balance the load supported by the forebody and check for zero moment about the C.G. With the aid of the afterbody dimensions listed in Table II, Figure 9 is plotted. Korvin-Kroukovsky, Savitsky, and Lehman (Referencell) have compiled ex-

perimental data and derived an empirical formula for plotting the longitudinal wave profile behind a vee-planing surface using the speed coefficient, angle of trim of the forebody, and aspect ratio as the entering parameters. Reference 11 states that the range of applicability of equation (10) should be restricted to values of the speed coefficient of not less than 3.0. It was assumed, however, that a speed coefficient of 2.62 was close enough to allow the use of the formulas. The following are the formulas used:

$$
\begin{aligned}
H &= H_o + H_\lambda \\
H_\lambda &= .0108\, \tau^{.34}\, (\lambda)(X) \\
H_o &= .0264 \left[\frac{X}{C_V^{.6}}\, \tau^{.7} \right]^2 - .00448 \left[\frac{X}{C_V^{.6}}\, \tau^{.7} \right]^{2.44}
\end{aligned}
\qquad (10)
$$

where H is the height above the keel baseline extended in beams and X is the distance aft of the step in beams. Table III shows the solution of the formula giving the height H also in inches to facilitate plotting.

It becomes necessary to introduce another correction. In the work at the Experimental Towing Tank, it was found that to make results predicted on the basis of wake survey agree with test results on the hull models, the wave height on the afterbody must be reduced to about 85%. This correction makes predicted wetted afterbody area agree with photographs of wetted afterbody areas obtained during actual test runs. After several trial and error computations, it was found that for the present case a wave

height reduction to 90% gave consistent results. In the region of intersection of the wave profile curve with afterbody bottom, the curve can be approximated by a straight line determined by the ordinates at the points (1) and (2) located at one and two beams aft of the step. In plotting these points, the ordinates were reduced to 90% of the value given in Table III. The angle measured between this line and the keel determines the angle of trim of the afterbody.

Afterbody Planing Data

Figure 5 shows the dimensions necessary for determining the angle of sweepback of the stagnation line defining the leading edge of the wetted area. This figure is based on Wagner's expanding plate theory, following References 6 and 10. The distance L_1 has the value

$$L_1 = \frac{b}{\pi} \frac{\tan \beta}{\tan \tau}$$

which leads to the sweepback angle defined as:

$$\tan \gamma = \frac{b/2}{L_1} .$$

Therefore

$$\tan \gamma = \frac{1}{\frac{2}{\pi} \frac{\tan\beta}{\tan \tau}} .$$

Knowing both the deadrise angle and the angle of trim, the required angle is found to be

$$\tan \gamma = .495$$

$$\gamma = 26^{\circ}20'$$

The angle γ is then laid out on Figure 9 starting at the leading

edge of the wetted length. The intersection of the constructed stagnation line with the chine line defines the beam of the afterbody used in all calculations requiring the beam of the afterbody. The length of the keel wetted length may be measured directly as

$$\ell_k = 198.5 \text{ in.} = 16.54 \text{ ft.}$$

and by geometry the mean wetted length equals

$$\ell_m = \frac{\ell_k}{2} = 8.27 \text{ ft.}$$

Again the aspect ratio of the afterbody may be computed as

$$\lambda = \frac{\ell_m}{b} = \frac{8.27}{5.83} \quad .$$

The speed coefficient is changed from that of the forebody by the inverse ratio of the square roots of the forebody and afterbody beam lengths, so that

$$(C_V)_A = (C_V)_F \left(\frac{10.0}{5.83}\right)^{\frac{1}{2}} = 2.62(1.31) = 3.43 \quad ,$$

where the beam value constructed above equals

$$b = 70 \text{ in.} = 5.83 \text{ ft.}$$

Therefore, the aspect ratio

$$\lambda = \frac{\ell_m}{b} = \frac{8.27}{5.83} = 1.42 \quad .$$

Knowing the angle of trim and aspect ratio, it is now possible to apply equations (6) and (7) to determine the lift coefficient for the afterbody. The lift coefficient for a flat planing surface is computed to be

$$C_{L_o} = \tau^{1.1} \left[.0120(1.191) + .0095(.171)\right]$$
$$= .0143 + .001625$$

$$C_{L_o} = \tau^{1.1} (.01593)$$
$$= .191$$

while the lift coefficient for a vee-planing surface is shown to be

$$C_{L_\beta} = .191 - .182(.370)$$
$$= .191 - .068$$
$$= .123 \quad .$$

Therefore, with the lift coefficient as computed, the load supported by the afterbody is

$$(\Delta)_A = .123 \left(\frac{1.937}{2}\right) (47)^2 (5.83)^2$$
$$= 8,950 \text{ lb.}$$

Using the load coefficient, the load supported by the forebody is added to the afterbody load to determine how closely it agrees with the load coefficient of the entire hull as specified at the start.

$$\Delta_F = .648(62.3) \times 10^4$$
$$= 40,300$$

$$(\Delta)_{total} = 40,300 + 8,950 = 49,250$$

$$(\Delta)_{total} = .8(62.3) \times 10^4 = 49,750 \quad .$$

In order to determine the center of pressure of the afterbody, equation (8) is again applied and the value of C_P computed as

$$C_P = .75 - \frac{1}{\frac{(3.43)^2}{(1.42)^{3/2}} + 2.42}$$

$$= .75 - \frac{1}{21.35 + 2.42} = .708 \quad .$$

In the case of the forebody, P was measured directly forward from the step. In the case of the afterbody, Reference 10 suggests that the distance P be measured as shown by Figure 6.

$$P = .708(8.27) = 5.86 \text{ ft.} = 70.3 \text{ in.}$$

From Figure 9, the distance L is 127.5 in., making L/2 = 63.75 in. The center of pressure is therefore 70.3 plus 63.75 or 134.05 in. from the end of the afterbody. Since the length of the afterbody is 328.5 in., the center of pressure acts at 328.5 minus 143.05 or 194.45 in. behind the step. The distance defined as ℓ_2 is then

$$\ell_2 = 16.2 \text{ ft.} + 3.67 \text{ ft.} = 19.87 \text{ ft.}$$

Moment Due to Resistance and Total Pitching Moment

The next step in analyzing the hull is to determine the pitching moment due to resistance. Resistance is computed for the model but plotted to full-scale values for convenience. Beginning with the Reynolds number which is low, the Prandtl-Karman relation is applied and the friction coefficient obtained. The friction coefficient so obtained is referred to wetted area and must be converted to the beam squared basis as shown. With the coefficient so obtained, it is then possible to determine the resistance in pounds. The same procedure is applied to the afterbody.

Forebody Frictional Resistance

$$(Re)_m = \frac{V \ell_m}{\nu}$$

$$= \frac{10 \ (12.5/22)}{1.08 \times 10^{-5}} = 5.26 \times 10^5 \qquad (11)$$

$$(C_F)_m = \frac{.074}{(Re)^{1/5}} = \frac{.0074}{1.394} = .00531 \qquad (12)$$

$$(C_R)_m = C_F \lambda \sec \beta = .00531(1.25)\left(\frac{1}{.927}\right)$$
$$= .00716 \qquad (13)$$

$$R = C_R \frac{\rho}{2} V^2 b^2 = 1630 \text{ lb.}$$

Afterbody Frictional Resistance

$$(Re)_m = \frac{10(8.27/22)}{1.08 \times 10^{-5}} = 3.48 \times 10^{+5}$$

$$(C_F)_m = \frac{.074}{(3.48)^{1/5} \times 10} = .00576$$

$$(C_R)_m = .00576(1.42)\left(\frac{1}{.883}\right)$$
$$= .00927$$

$$R = .00927\left(\frac{1.937}{2}\right)(47)^2(5.83)^2$$

$$= 672 \text{ lb.}$$

The total frictional resistance is then the sum of the forebody and the afterbody resistance. In the process of determining the forces on the hull, it was found that the value of resistance was too low and therefore all values of resistance were increased by 25%. This in effect accounts for roughness and other unknown variations. When the resistance is increased by 25%, the result is found to agree very well with the values of resistance shown in Reference 9. Therefore the total frictional resistance is found to be

$$(R)_T = 1630 + 672$$
$$= 2302$$

$(R)_T = 1.25(2302) = 2880$.

With all the forces computed for the entire hull for the condition being considered, it is now possible to compute the moments about the C.G. of the hull. Forces considered are taken perpendicular to the keel reference line as shown in Figure 7. The inclination of the afterbody force to the vertical is considered small and its horizontal component is therefore neglected. The sum of the moments yields

$$41,300(4.99) = 2880(10) + 8,950(19.87)$$

$$206,000 = 28,800 + 177,800$$

$$206,000 \cong 206,600 \quad .$$

Therefore the sum of the moments about the C.G. does indicate the initial condition of zero moment about the C.G. to a very good approximation. The satisfactory agreement of both summations of forces and of moments is now taken as a confirmation that the computed ℓ_1 and ℓ_2 are correct.

Unbalance of Loads on Two Sides of the Hull

In order to arrive at an analytical expression or procedure for the determination of the transverse forces on a hull in the yawed condition, it is necessary to associate a change in the effective angle of trim on each side of the hull with a given angle of yaw. From Figure 8, the vee-bottom planing surface is considered to be equivalent to a wing with dihedral. When the planing surface is given a positive yaw, the force diagram shown for the starboard side indicates that there will be a decrease

in the angle of trim acting on that side, the magnitude of which will be

$$V\Delta\alpha = V \sin \Upsilon \sin \beta$$

$$\Delta\alpha = \Upsilon \sin \beta \text{ (for small yaw angles)} \quad . \qquad (14)$$

There will be an increase in the trim angle on the port side for the same positive yaw angle of the same magnitude.

Some expression must be found that will allow the increase in lift to be computed if the change in the angle of trim is known. Equations (6) and (7) may be changed slightly in view of the assumption that for small yaw angles the center of pressure and the aspect ratio remain constant. The expression for the original trim is then altered to include a small change in trim.

$$C_{L_o} = \tau^{1.1} \left[.0120 \lambda^{\frac{1}{2}} + .0095 \left(\frac{\lambda}{C_V} \right)^2 \right]$$

$$= k_1 \tau^{1.1}$$

$$C_{L_\beta} = C_{L_o} - .0065(\beta) C_{L_o}^{.6}$$

$$= C_{L_o} - k_2 C_{L_o}^{.6}$$

$$C_{L_\beta} = k_1 \tau^{1.1} - k_2 (k_1 \tau^{1.1})^{.6}$$

The original lift is defined as $(C_{L_\beta})_1$ and the new lift due to an increase in the trim as $(C_{L_\beta})_2$.

$$(C_{L_\beta})_1 = k_1 \tau^{1.1} - k_2 (k_1 \tau^{1.1})^{.6}$$

$$k(C_{L_\beta})_1 = \Delta_o$$

$$k(C_{L_\beta})_2 = \Delta$$

where

$$k = \frac{\rho}{2} V^2 b^2$$

$$(C_{L_\beta})_2 = k_1(\tau + \Delta\tau)^{1.1} - k_2\left[k_1(\tau + \Delta\tau)^{1.1}\right].6 \quad .$$

By the binomial expansion

$$(\tau + \Delta\tau)^{1.1} = \tau^{1.1} + 1.1\,\tau^{.1}\Delta\tau + \frac{1.1(.1)}{2!}\tau^{-.9}(\Delta\tau)^2 + \ldots$$

Neglecting the third term as being of higher order,

$$(\tau + \Delta\tau)^{1.1} = \tau^{1.1} + 1.1\tau^{.1}\,\Delta\tau \quad .$$

Therefore,

$$(C_{L_\beta})_2 = k_1\tau^{1.1} + k_1(1.1)\tau^{.1}\,\Delta\tau - k_2\left[k_1\tau^{1.1} + k_1(1.1)\tau^{.1}\Delta\tau\right].6$$

The expansion of the term in the brackets gives

$$k_2\left[k_1\tau^{1.1} + k_1(1.1)\tau^{.1}\Delta\tau\right].6 = k_2(k_1\tau^{1.1}).6\left[1 + (1.1)(.6)\frac{\Delta\tau}{\tau} + \frac{(1.1)(.6)(-.4)}{2}\left(\frac{\Delta\tau}{\tau}\right)^2 + \ldots\right]$$

Again the third term of the expansion is neglected as being of higher order. Therefore,

$$(C_{L_\beta})_2 = k_1\tau^{1.1} + k_1(1.1)\tau^{.1}\Delta\tau - k_2(k_1\tau^{1.1}).6\left[1 + (1.1)(.6)\frac{\Delta\tau}{\tau}\right]$$

If the value for $(C_{L_\beta})_1$ is substituted,

$$(C_{L_\beta})_2 = (C_{L_\beta})_1 + \frac{\Delta\tau}{\tau}\left[k_1(1.1)\tau^{1.1} - (1.1)(.6)k_2(k_1\tau^{1.1}).6\right]$$

Multiplying through by k to obtain the loads gives

$$\Delta = \Delta_o + k\,\frac{\Delta\tau}{\tau}\left[k_1(1.1)\tau^{1.1} - (1.1)(.6)k_2(k_1\tau^{1.1}).6\right] .$$

The expression in the brackets is, to a very close approximation,

the value of $(C_{L_\beta})_1$, since for relatively small values of trim the negative term in the brackets is quite small and not seriously affected by the factor of 0.6. Therefore the complete expression:

$$\Delta = \Delta_o + \Delta_o \frac{\Delta\tau}{\tau}$$

or

$$\Delta = \Delta_o \left(\frac{\tau \pm \Delta\tau}{\tau} \right) \qquad (15)$$

The $\pm$ sign in equation (15) is put in so as to include increases or decreases in trim since the same result would have been obtained had the derivation been considered for a decrease in the trim angle. Equation (15) states that new load on a planing surface is found by multiplying the original load by the ratio of the new trim angle to the old trim angle.

Lateral Force Computations

Equations (3) and (4) gave expressions for determining the value of the forces F_1 and F_2 acting at the forebody and afterbody center of pressures. The hull for Condition 1 as specified in Table IV has the following value for the static directional stability derivatives:

$$\left.\begin{aligned} Y'_\beta &= .229 \\ N'_\beta &= -.172 \end{aligned}\right\} \quad \text{slopes per radian} \quad .$$

Under the assumption that the wetted length remains constant for small yaw angles and that the static derivatives reported are constant or linear out to 1^o yaw angle, the value of the forces may be computed on the basis that the angle of yaw is 1^o.

$\ell_1 = 4.99$ ft. $\quad Y' = Y'_\beta \beta = .004$ $\quad b = 10$ ft.

$\ell_2 = 19.87$ ft. $\quad N' = N'_\beta \beta = -.003$ $\quad N'b = -.03$

$\ell_1 + \ell_2 = 24.86$ ft. $\quad V = 47$ ft./sec. $\quad \ell_2 Y' = .0795$

$\ell_1 Y' = .02$

$$F_1' = \frac{\ell_2 Y' + N'b}{\ell_1 + \ell_2} = \frac{.0795 - .03}{24.86} = 1.99 \times 10^{-3}$$

$$F_1 = 1.99 \times 10^{-3} \left(\frac{1.937}{2}\right) (47)^2 (10)^2$$

$$F_1 = 424 \text{ lb.}$$

$$F_2' = \frac{\ell_1 Y' - N'b}{\ell_1 + \ell_2} = \frac{.02 + .03}{24.86} = 2.01 \times 10^{-3}$$

$$F_2 = 2.01 \times 10^{-3} \left(\frac{1.937}{2}\right) (47)^2 (10)^2$$

$$F_2 = 428 \text{ lb.}$$

Therefore, for the condition specified, the static derivatives will have the value shown if the forces computed act at the centers of pressure at the distances shown when the hull is placed at an angle of yaw of 1°.

With the forces known that must act in order to produce a given static stability, a correlation must be made and shown to be valid if the static stability is to be predicted from the method so far presented. Equation (15) is therefore used to obtain the changes in loads due to specified yaw angles. A yaw of 1° is taken as standard. Thus the change in trim will be:

$$\Delta\tau = 0.374^\circ$$

for the forebody deadrise of 22°. Figure 11(a) shows how the force vectors are constructed. The total load on the forebody is considered to be composed of two vectors each equal to one-half the total force acting at the center of pressure. Each vector acts on one side of the vee surface. For a positive yaw, the diagram shows that the vector on the right side has been increased by the relation of equation (15), while the force vector on the left has been decreased. The designation right and left refers to the position of vectors as viewed when looking directly at Figure 11 and is opposite to the designation which would be used by the pilot sitting in the hull and looking out ahead of the hull. The former system is used for direct comparison with Figure 11. When the horizontal components are computed using the tangent relation of the deadrise angle, an unbalanced force to the left is observed. The value of 470 obtained agrees very well with the force of 424 that was previously shown must exist.

$$(\Delta)_{right} = \frac{41,300}{2}\left(\frac{12.6 + .374}{12.6}\right) = 21,250$$

$$(\Delta)_{left} = \frac{41,300}{2}\left(\frac{12.6 - .374}{12.6}\right) = 20,050 \quad .$$

The horizontal force is then

$$\tan 22^\circ\ (21,250) = 8,570 \text{ lb.}$$

$$\tan 22^\circ\ (20,050) = \underline{8,100} \text{ lb.}$$

$$\text{Net Force} \qquad 470 \text{ lb.}$$

The same procedure is used for the afterbody, and the force diagrams on the right-hand side of Figure 11(a) show that

for agreement, the force due only to change in trim angle is insufficient. The value is computed as 210 lb. when from the analysis of the static derivatives it was seen that a force of 428 lb. must act on the afterbody.

$$\Delta\tau = \sin\gamma \sin\beta$$

$$\Delta\tau = 0.47^{\circ} \qquad (28^{\circ} \text{ deadrise})$$

$$(\Delta)_R = \frac{8,950}{2}\left(\frac{9.6 + 0.47}{9.6}\right) = 4,700$$

$$(\Delta)_L = \frac{8,950}{2}\left(\frac{9.6 - 0.47}{9.6}\right) = 4,250$$

$$\tan 28^{\circ}\ (4,700) = 2,200 \text{ lb.}$$

$$\tan 28^{\circ}\ (4,250) = \underline{1,990} \text{ lb.}$$

Net Force 210 lb.

Therefore it is obvious that some other force must be added to provide satisfactory agreement. References 11 and 12 contain profiles of the transverse wave shapes for a vee-planing surface. Unfortunately, no empirical relation exists for the transverse wave as is the case with the longitudinal wave profile. Therefore it was not possible to construct a transverse wave based on Condition 1 of Table IV. Since no conditions in References 11 and 12 exactly duplicated Condition 1, Figure 27 of Reference 11 was chosen for the closest agreement. By consulting Figure 27 of Reference 11, it will be seen that the point where the afterbody center of pressure acts is located somewhere between one and two beams aft of the step. It will be observed that the lateral displacement of the hull at this point results in the fact that the

wake is not symmetrical with respect to it and the water level (not yet disturbed by the hull) is located at different heights above the chine on the port and starboard sides. This fact can be simply interpreted as the mean lateral inclination at the water surface. Because of this inclination, an added horizontal force will be created which will add to the force already existing due to the change in the effective angle of trim of the afterbody.

In the present work, a short-afterbody hull is being considered at a small angle of yaw, and the effect of the wake has been found to be stabilizing. If the angle of yaw had been large enough for the afterbody to ride over the wave crest, the effect would have changed from a stabilizing to a destabilizing one. Likewise, if a long-afterbody hull had been used, it would have been found to ride on a roach, so that a small displacement would have moved it towards the hollow which forms on the side of the roach at this distance from the step. Again the effect would have been destabilizing, and the directional stability difficulties with the long-afterbody hull are well-known.

At 1^{o} angle of yaw, the lateral displacement of the hull centerline at the location of the center of pressure, (i.e., 19.87 ft.) aft of the C.G. is

$$\Delta y = \frac{19.87}{57.3} = .347$$

or .035 of the forebody beam. At this small distance from the centerline, the wave slope is too small to be measured on the

diagrams of Reference 11. Therefore the procedure shown below is used:

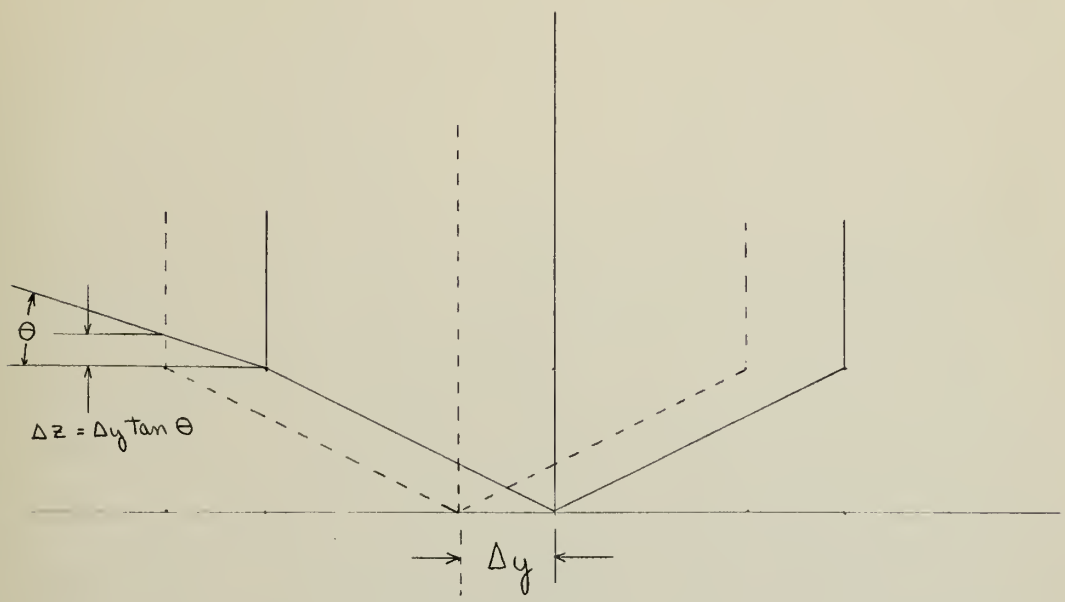

The angle of the wave is measured at the chine where it is found to be 19.5° by average between the values at one and two beams aft of the step. The desired slope is then computed to be

$$\frac{2\Delta Z}{\text{afterbody beam}} = \frac{2\,[\tan 19.5^{\circ}(.347)]}{5.83} = .0422$$

The afterbody lift force of 8,950 by acting on the slope of .0422 adds a lateral force of

$$8{,}950(.0422) = 378 \text{ lb.}$$

The test conditions for which the diagrams are given in Reference 11 do not correspond directly to the conditions of the hull analyzed herein. The following table gives the comparison:

Nearest Conditions from Reference 11	Conditions of Present Analysis
$\tau = 12^\circ$	$\tau = 12.6^\circ$
$\beta = 30^\circ$	$\beta = 22^\circ$
$C_\Delta = .73$	$C_\Delta = .648$
$C_V = 3.69$	$C_V = 2.63$

The number of test points in Reference 11 did not permit exact extrapolation, and certain bold assumptions had to be made. It was assumed that the differences in C_Δ and in trim τ were small enough to be neglected. It was further assumed that the transverse slope of the wave near the centerline of the wake is proportional to the angle of deadrise. This left only the effect of the speed coefficient to be extrapolated. It appeared from the study of the diagrams of Reference 11 that the slopes are proportional to 0.9 of the ratio of the C_V involved. Since the lateral force is proportional to the slopes, it becomes in this case

$$378 \left(\frac{1}{\frac{3.69}{2.63} \times .9} \right) \frac{22}{30} = 220 \text{ lb.}$$

The correct horizontal force is then the addition of 210 lb. plus 220 lb. or a total force of 430 lb. which is now in good agreement with the force of 428 lb. which was shown had to exist in order that the static stability derivatives quoted should exist.

Static Directional Stability

It is now possible to obtain the stability derivatives

knowing the forces created on the hull during a 1^{o} angle of yaw. The two forces are added together for the total transverse force, made nondimensional, and therefore as such represent the slope of transverse force curve vs. yaw angle for small angles of yaw. The moments are computed from the transverse forces acting at the arms ℓ_1 and ℓ_2, made nondimensional, and thereby represent the slope of the yawing moment vs. angle of yaw curve.

$$\frac{\partial Y'}{\partial \beta} = \frac{2\,(470 + 430)}{(1.937)(2,210)(100)}$$

$$= +.00421 \text{ per degree}$$

$$= +.241 \text{ per radian}$$

$$\frac{\partial N'}{\partial \beta} = \frac{2\left[470(4.99) - 430(19.87)\right]}{1.937(2,210)(100)}$$

$$= \frac{-2(6,215)}{1.937(2,210)(1,000)}$$

$$= -.00291 \text{ per degree}$$

$$= -.167 \text{ per radian}$$

It will be observed that the above values of the static stability derivatives have been obtained on the basis of hull geometry, the empirical relations for the lift of planing surfaces, and the data of the wake survey without any reference to the direct stability tests. It will be of interest now to compare these values with the values obtained by direct test in Reference 7.

	$\partial Y'/\partial \beta$	$\partial N'/\partial \beta$
By computation	.241	-.167
By direct test	.229	-.172

The correlation now appears complete and for the condition of the hull shown the mathematical method of determining the static stability derivatives gives excellent agreement with test results. A summary of the method now follows:

1. For any condition specified for trim, speed coefficient, load coefficient, and trimming moment, the hull is analyzed for the vertical forces acting on the forebody and afterbody and the arms ℓ_1 and ℓ_2 from the position of the C.G.
2. A 1° angle of yaw is given the hull and formulas (14) and (15) are applied to solve for the horizontal forces existing on the forebody and afterbody as shown in Figure 11.
3. The horizontal force on the afterbody is corrected by considering transverse wave shapes from References 11 and 12 and the additional force these wave shapes add.
4. With the horizontal forces acting at ℓ_1 and ℓ_2, the static derivatives may be computed for the 1° yaw angle, giving the slopes of the desired curves per degree yaw. These may then be converted to radian measure.

The mathematical treatment is not complete until the ana-

lysis has been made which produces the expressions and equations necessary to convert the static stability derivatives into dynamic stability derivatives.

Rotary Stability Derivatives

Returning to equation (2), the moment N may be expressed as

$$N = \ell_1 \left[\frac{\ell_2 Y + N}{\ell_1 + \ell_2} \right] - \ell_2 \left[\frac{\ell_1 Y - N}{\ell_1 + \ell_2} \right] \qquad (16)$$

which in reality is an identity for the yawing moment N and yields

$$N \equiv N \quad .$$

However, equation (16) is used to derive an expression for the rotary stability derivatives by giving the hull in Figure 1(a) an angular velocity "r" about the Z-axis. If the angular velocity "r" is referred to the C.G., such an angular velocity will create a linear velocity $r\ell_1$ at the forebody center of pressure and a velocity $r\ell_2$ at the afterbody center of pressure.

By definition:

$$N = N'_\beta \beta \frac{\rho}{2} V^2 b^3 \qquad (17)$$

and

$$Y = Y'_\beta \beta \frac{\rho}{2} V^2 b^2 \quad . \qquad (18)$$

The effect of giving the hull an angular velocity is to add or subtract from the forces resulting from an initial yawing angle another yaw angle $\Delta\beta$ which for small angles on the forebody has the value $r\ell_1/V$ and on the afterbody $r\ell_2/V$. The effec-

tive angles of yaw are then:

$$\left.\begin{aligned}(\beta)_{\text{forebody}} &= \beta_o - \frac{r\ell_1}{V} \\ (\beta)_{\text{afterbody}} &= \beta_o + \frac{r\ell_2}{V}\end{aligned}\right\} \qquad (19)$$

Substituting equations (17), (18), and (19) into equation (16) gives

$$N = \ell_1\left[\frac{\ell_2 Y'_\beta\left(\beta_o - \frac{r\ell_1}{V}\right)\frac{\rho}{2}V^2b^2 + N'_\beta\left(\beta_o - \frac{r\ell_1}{V}\right)\frac{\rho}{2}V^2b^3}{(\ell_1+\ell_2)}\right]$$

$$-\ell_2\left[\frac{\ell_1 Y'_\beta\left(\beta_o + \frac{r\ell_2}{V}\right)\frac{\rho}{2}V^2b^2 - N'_\beta\left(\beta_o + \frac{r\ell_2}{V}\right)\frac{\rho}{2}V^2b^3}{(\ell_1+\ell_2)}\right]$$

Clearing brackets:

$$N = \frac{\ell_1\ell_2 Y'_\beta\beta_{o2}\frac{\rho}{2}V^2b^2 + \ell_1 N'_\beta\beta_{o2}\frac{\rho}{2}V^2b^3 - \ell_2\ell_1 Y'_\beta\beta_{o2}\frac{\rho}{2}V^2b^2}{\ell_1+\ell_2}$$

$$+\frac{\ell_2 N'_\beta\beta_{o2}\frac{\rho}{2}V^2b^3}{\ell_1+\ell_2}$$

$$+\frac{-\ell_1\ell_2 Y'_\beta\left(\frac{r\ell_1}{V}\right)\frac{\rho}{2}V^2b^2 - \ell_1 N'_\beta\left(\frac{r\ell_1}{V}\right)\frac{\rho}{2}V^2b^3}{\ell_1+\ell_2}$$

$$+\frac{-\ell_2\ell_1 Y'_\beta\left(\frac{r\ell_2}{V}\right)\frac{\rho}{2}V^2b^2 + \ell_2 N'_\beta\left(\frac{r\ell_2}{V}\right)\frac{\rho}{2}V^2b^3}{\ell_1+\ell_2}$$

$$N = \frac{N'_\beta\beta_{o2}\frac{\rho}{2}V^2b^3(\ell_1+\ell_2)}{(\ell_1+\ell_2)} + \Delta N$$

$$= N'_\beta\beta_{o2}\frac{\rho}{2}V^2b^3 + \Delta N \quad .$$

where ΔN is defined as

$$\Delta N = \frac{-\ell_1 \ell_2 Y'_\beta \left(\frac{r\ell_1}{V}\right) \frac{\rho}{2} V^2 b^2 - \ell_1 N'_\beta \left(\frac{r\ell_1}{V}\right) \frac{\rho}{2} V^2 b^3}{\ell_1 + \ell_2}$$

$$\frac{-\ell_1 \ell_2 Y'_\beta \left(\frac{r\ell_2}{V}\right) \frac{\rho}{2} V^2 b^2 + \ell_2 N'_\beta \left(\frac{r\ell_2}{V}\right) \frac{\rho}{2} V^2 b^3}{\ell_1 + \ell_2}$$

Using dimensionless coefficients:

$$N' = N'_\beta \beta_o + \Delta N' \quad .$$

The resulting moment on the hull is the sum of the moment due to initial yaw angle plus some change due to the angular velocity. For the purposes herein, interest is concentrated in the $\Delta N'$ created by the angular velocity, that is, for zero initial yaw angle.

$$\Delta N' = \frac{-\ell_1 \ell_2 Y'_\beta \left(\frac{r\ell_1}{Vb}\right) - \ell_1 N'_\beta \left(\frac{r\ell_1}{V}\right)}{\ell_1 + \ell_2}$$

$$+ \frac{-\ell_1 \ell_2 Y'_\beta \left(\frac{r\ell_2}{Vb}\right) + \ell_2 N'_\beta \left(\frac{r\ell_2}{V}\right)}{\ell_1 + \ell_2}$$

Differentiate with respect to the dimensionless parameter $r' = \frac{rb}{V}$:

$$N'_r = \frac{-\ell_1 \ell_2 Y'_\beta \left(\frac{\ell_1}{b^2}\right) - \ell_1 N'_\beta \left(\frac{\ell_1}{b}\right)}{\ell_1 + \ell_2}$$

$$+ \frac{-\ell_1 \ell_2 Y'_\beta \left(\frac{\ell_2}{b^2}\right) + \ell_2 N'_\beta \left(\frac{\ell_2}{b}\right)}{\ell_1 + \ell_2}$$

$$N'_r = \frac{\frac{-l_1 l_2 Y'_\beta}{b^2}(l_1 + l_2) + \frac{N'_\beta}{b}(l_2^2 - l_1^2)}{l_1 + l_2}$$

$$N'_r = \frac{-l_1 l_2 Y'_\beta}{b^2} + \frac{N'_\beta}{b}(l_2 - l_1) \quad . \tag{20}$$

This represents the equation necessary to determine analytically the rotary derivatives, knowing the static derivatives. The quantities l_1 and l_2 are determined for the planing conditions, assuming that for small disturbances from a straight course the forces F_1 and F_2 continue to act at the centers of pressure of the forebody and afterbody.

Using equation (1),

$$Y = F_1 + F_2$$

and also

$$Y = \frac{N + l_2 Y}{l_1 + l_2} + \frac{l_1 Y - N}{l_1 + l_2} \quad .$$

This again is an identity in Y ; however, if once again equations (17), (18), and (19) are restorted to, the following is obtained:

$$Y = \frac{N'_\beta \left(\beta_o - \frac{r l_1}{V}\right) \frac{\rho}{2} V^2 b^3 + l_2 Y'_\beta \left(\beta_o - \frac{r l_1}{V}\right) \frac{\rho}{2} V^2 b^2}{l_1 + l_2}$$

$$+ \frac{l_1 Y'_\beta \left(\beta_o + \frac{r l_2}{V}\right) \frac{\rho}{2} V^2 b^2 - N'_\beta \left(\beta_o + \frac{r l_2}{V}\right) \frac{\rho}{2} V^2 b^3}{l_1 + l_2}$$

from which

$$Y = \frac{N'_\beta \beta \beta_{o2} \frac{\rho}{2} V^2 b^3 - N'_\beta \left(\frac{r \ell_1}{V}\right) \frac{\rho}{2} V^2 b^3 + \ell_2 Y'_\beta \beta_{o2} \frac{\rho}{2} V^2 b^2}{\ell_1 + \ell_2}$$

$$+ \frac{- \ell_2 Y'_\beta \left(\frac{r \ell_1}{V}\right) \frac{\rho}{2} V^2 b^2 + \ell_1 Y'_\beta \beta_{o2} \frac{\rho}{2} V^2 b^2 + \ell_1 Y'_\beta \left(\frac{r \ell_2}{V}\right) \frac{\rho}{2} V^2 b^2}{\ell_1 + \ell_2}$$

$$+ \frac{- N'_\beta \beta_{o2} \frac{\rho}{2} V^2 b^3 - N'_\beta \left(\frac{r \ell_2}{V}\right) \frac{\rho}{2} V^2 b^3}{\ell_1 + \ell_2} \quad .$$

Making results nondimensional

$$Y' = Y'_\beta \beta_o + \Delta Y'$$

where

$$\Delta Y' = \frac{- N'_\beta \left(\frac{r \ell_1 b}{V}\right) - \ell_2 Y'_\beta \left(\frac{r \ell_1}{V}\right)}{\ell_1 + \ell_2}$$

$$+ \frac{\ell_1 Y'_\beta \left(\frac{r \ell_2}{V}\right) - N'_\beta \left(\frac{r \ell_2 b}{V}\right)}{\ell_1 + \ell_2} \quad .$$

The same situation exists for transverse forces as for moments. That is, the total Y force is the sum of effects from initial yaw angle and added angular velocity. Interest is again centered only in that transverse force due to angular velocity. Therefore taking the expression for $\Delta Y'$ and differentiating with respect to the dimensionless parameter $r' = \frac{rb}{V}$ gives:

$$Y'_r = \frac{-N'_\beta \ell_1 - \ell_2 Y'_\beta \left(\frac{\ell_1}{b}\right) + \ell_1 Y'_\beta \left(\frac{\ell_2}{b}\right) - N'_\beta \ell_2}{\ell_1 + \ell_2}$$

$$Y'_r = - N'_\beta \quad . \tag{21}$$

ANALYSIS FOR CONDITIONS 2 AND 3

The analysis of the hull for a speed coefficient of 2.62 was a straightforward application of the equations for lift of a prismatic vee-planing surface, the equations for center of pressure measurements found in Reference 10, and the shape of the longitudinal wave profile as computed in Reference 11. One of the limiting conditions in Reference 11 is that the speed coefficient be no less than 3. Difficulty was encountered when the hull was analyzed for speed coefficients of 2.46 and 2.34. The value in equation (10) of H_o contributes the largest portion of the computed wave height. The following values of the trim and speed coefficient as entering variables for the three conditions are noted:

Condition	τ	C_V	$\tau^{.7}$	$\tau^{.34}$	$C_V{}^{.6}$	$\tau^{.7}/C_V{}^{.6}$
1	12.6°	2.62	5.88	2.366	1.783	3.3
2	11.2°	2.46	5.42	2.275	1.716	3.16
3	10.5°	2.34	5.18	2.225	1.665	3.11

It has been mentioned previously that at a C_V of 2.62, the formulas for the longitudinal wave profile were used beyond the range of the wake tests which went down only as low as $C_V = 3.0$. At $C_V = 2.46$ and 2.34, this extrapolation had to extend so much further that the trial applications indicated that it was not possible to obtain the proper wetted length of the afterbody by this means. In absence of the actual wake data,

therefore, the following alternate procedure was adopted. It was clear from the basic theory that the forebody load will be decreasing and the afterbody load will be increasing with a decrease of the speed coefficient C_V . In Condition 1, the forebody load was found to be 81% of the total load. It is assumed now that the forebody load becomes 75% of the total load for Condition 2 and 70% for Condition 3. Using the trim angle data obtained from the test and the planing relations formula, the forebody wetted length and the position of the center of pressure were computed. The afterbody load was taken as the difference between the total and the assumed forebody load. The necessity to obtain the balance of forces and moments therefore dictated a definite value for the distance from the C.G. to the position of the afterbody center of pressure. A suitable set of values for the afterbody wetted length and afterbody effective angle of trim was obtained by trial and error, so that the frictional resistance of the afterbody was properly accounted for in the balance of moments. In absence of the available wake data for the low values of C_V , the above procedure can be considered as the best substitute.

It was assumed that the transverse wave profiles can be extrapolated to the low values of C_V in the same way as it has been shown in detail for Condition 1. With the mean lateral slope of the wave obtained in this way and with the values of the afterbody angle of trim as obtained as explained above, the

changes of the effective angle of trim on the two sides of the hull and the resultant lateral force were readily computed. The results of these computations for Conditions 2 and 3 are given in Appendix II. A recapitulation of all the hydrodynamic planing characteristics is contained in Table V for the three conditions considered. Figure 9 contains the afterbody wetted areas for each of the three speed coefficients investigated for comparison purposes. Figure 11 contains the hull force diagrams for the three conditions investigated.

MATERIAL AND TEST PROCEDURE

The model used in the tests was that of a conventional large flying boat designated as Stevens Model 406. The model dimensions appear in Tables I and II. A diagrammatic sketch in Figure 2 shows the essential parts of the standard seaplane yawing apparatus which was prepared using Reference 13 as a guide. The carriage on which the model was mounted allowed for freedom in trim, heave, and yaw. Freedom in heave was necessary to allow for correct wetted length although the heave for each run was not recorded. The apparatus was equipped with an unloader which permitted any desired load on the water to be obtained regardless of the weight of the model. The yawing tests in the present work were run at a constant load coefficient and at zero heel angle although it was possible to vary the heel angle. Angle of trim and yawing angle were recorded for each run.

No apparatus existed in Tank No. 1 for the direct determination of the sidewise force due to yaw angle. Therefore an indirect method was used which proved fairly satisfactory. The moments about the C.G. and about an arbitrary point 3.56 in. forward of the C.G. were computed at the same fixed trim which coincided with the free-to-trim angle obtained for zero yaw angle. The moment about the point forward of C.G. minus the moment about the C.G. is equal to the sidewise force acting at the C.G. times the distance between the two points. This equation may be made nondimensional and differentiated with respect

to β , which will lead to the following result:

$$N_2 - N_1 = - Y X$$

$$N_2' - N_1' = - Y' X'$$

$$\frac{\frac{\partial N_2'}{\partial \beta} - \frac{\partial N_1'}{\partial \beta}}{X'} = - \frac{\partial Y'}{\partial \beta}$$

where

N_1 = dimensional force about the C.G.

N_1' = nondimensional force about the C.G.

N_2 = dimensional force about forward pivot

N_2' = nondimensional force about front pivot

X = dimensional distance between pivots

X' = nondimensional distance between pivots

Therefore, the model was equipped with two sets of pivots, the distance between the pivots being 3.56 in. The model was balanced around the rear pivots where the C.G. was located 2.00 in. forward of the step and 6 in. above the keel. This corresponded to a full scale C.G. position of 3.67 ft. forward of the step and 11.0 ft. above the keel. The position of the model in the carriage is shown in Figure 3.

It was necessary to make three runs to record all the data. The first run in the free-to-trim attitude made use of the rear pivots of the model where the C.G. of the model was established. A standing yaw was recorded, the model sent down the tank at a predetermined speed, and the running yaw recorded

as well as the trim. The difference in the standing and running yaw was multiplied by the spring calibration to give the moment in inch-pounds (calibrated in inch-pounds per degree change in yaw angle). The resulting moment was made dimensionless and plotted as yawing moment vs. running yaw angle. The springs which restrained the yawing motion of the model were available in four varying degrees of stiffness. The calibrations for the two used are shown in Figure 12. These two springs were distinguished by red and yellow paint. A dashpot was also included which damped out oscillations in yaw. The spring was located 15.5 in. from the yawing pivot.

Reference 2 contains a good description of the procedure sometimes followed when hulls exhibit directional instability. The method consists of actually pushing the model while running in order to get points on the curve which would otherwise be impossible to obtain due to a combination of instability and spring stiffness. Figure 4 shows the relation between standing and running yaw. Since the yaw angle could be read only to the nearest 0.1, springs were interchanged at various times to improve the scatter of the points on the curve.

Once the running trim angle was determined, the model was locked in trim at the free-to-trim angle for zero yaw and run again for angles of yaw from 6° port to 6° starboard. Immediately following this, the model was locked at the same angle of trim on the front pivot and runs were again made covering the same

range of yaw angles. The trim lock was of simple friction type.

All the testing was conducted in Tank No. 1 of the Experimental Towing Tank, Stevens Institute of Technology. The tank is 95 ft. long and of semi-circular cross section with an added dock section 6 ft. long to facilitate preparation and mounting of the model. The carriage is suspended from a monorail which follows the centerline of the tank. Power is received from a towing line which is driven by a multiple-diameter cone pulley. Provisions are made for further varying speed by interchangeable gear boxes. Power to the towing line is supplied by direct current until the model is up to speed at which time an A.C. synchronous motor cuts in to operate the carriage at a constant speed.

The water level of the tank had to be carefully controlled so that the carriage would have no restriction in heave. The water level for fixed trim was generally lower than for the free-to-trim case. The criterion of correct freedom in heave was that the carriage horizontal balancing arm should extend slightly above the horizontal position when the model was at rest in the dock.

Prior to running, all three test conditions shown in Table IV were checked with Reference 14 in order to ensure that the hull was not in the porpoising range.

TEST RESULTS

Tables VI through XIV tabulate the results of the tank yawing tests, and these results are shown as moment vs. yaw angle curves in Figures 13 through 21. Figure 12 shows the spring calibration for the two springs used for determining the value of yawing moment. Table IV gives the three conditions used in the present investigation. Figure 10 shows a photograph of a typical run as obtained during the tank testing program. Table XV and Figure 22 are considered to constitute the final results, for, in these, a comparison is made of both the computed and test values obtained.

The three test conditions chosen correspond to conditions which were predicted to exist just beyond the unstable range. That is for a C_V less than 2.31, the model becomes unstable as shown on a composite static stability chart for a similar typical hull configuration. The test results show that with a decreasing speed coefficient, the hull becomes increasingly stable. However, the stability is represented by three stable branches of the curve with discontinuities existing in the vicinity of 5° port and starboard. For the lowest speed coefficient, the hull was the most stable, with the discontinuity between the three stable branches existing at about 3° port and starboard. It was predicted in the mathematical analysis that a decrease in the speed coefficient would lead to an increase in stability. However, the stability predicted for the lowest speed coefficient

was approximately one third less than the static stability found by test, in the case of yawing moment vs. yaw angle.

All the free-to-trim moment curves for the three conditions check favorably with similar curves previously reported (Reference 2). Difficulty was encountered in setting the model at zero yaw angle. No accurate apparatus exists in Tank No. 1 for such a procedure. So much water had to be let out of the tank that the measuring device used had to butt against the curved sides of the dock. The red and yellow springs were constantly being changed in order to obtain better curves. Each time the spring was changed, the point of zero yaw was shifted. The fact that the zero yaw calibration was not good has shown up in the moment curves as a horizontally displaced curve. The apparatus was set at zero heel but it was noted that quite a bit of play existed in the pivot support which was equivalent to inducing an angle of heel on the model. Figure 18 is the only curve which shows a vertically displaced axis due to some induced heel angle. The displacements of the axis in either direction for these tests were considered small enough to have no effect on the slope of the moment curve for zero yaw angle.

Concern in moment curves for the fixed trim case was centered in small angles of yaw. Since the change in trim angle was not too large for small angles of yaw, fixed trim was taken at the value of trim for zero yaw angle. Using the method already suggested of subtracting the slopes of the moment curves for

front and rear pivots at the same fixed trim, the following are the solutions for transverse force vs. yaw for the three conditions tested:

$C_V = 2.63$

Front pivots $\frac{\partial N_2'}{\partial \beta} = - .0075$

Back pivots $\frac{\partial N_1'}{\partial \beta} = - .0050$

$$\frac{\partial N_2'}{\partial \beta} - \frac{\partial N_1'}{\partial \beta} = - \frac{\partial Y'}{\partial \beta} X'$$

$$- \frac{\partial Y'}{\partial \beta} = \frac{- .0075 + .0050}{.653}$$

$$\frac{\partial Y'}{\partial \beta} = .00383/\text{degree}$$

$$= .219/\text{radian}$$

$C_V = 2.46$

Front pivots $\frac{\partial N_2'}{\partial \beta} = -.0052$

Back pivots $\frac{\partial N_1'}{\partial \beta} = -.0020$

$$- \frac{\partial Y'}{\partial \beta} = \frac{- .0052 + .0020}{.653}$$

$$\frac{\partial Y'}{\partial \beta} = .0049/\text{degree}$$

$$= .281/\text{radian}$$

$C_V = 2.34$

Front pivots $\frac{\partial N_2'}{\partial \beta} = -.018$

Back pivots $\frac{\partial N_1'}{\partial \beta} = -.013$

$$-\frac{\partial Y'}{\partial \beta} = \frac{-.018 + .013}{.653}$$

$$\frac{\partial Y'}{\partial \beta} = .00766/\text{degree}$$

$$= .439/\text{radian} \quad .$$

MISCELLANEOUS

The testing program in Tank No. 1 began with Condition 1, wherein the speed coefficient was 2.63. This was the case where the best agreement was desired in order to form a basis for the subsequent analysis. Unfortunately, due to the lack of previous experience with the apparatus and tank testing techniques, the experimental data in this first condition were obtained with a larger amount of difficulty and with less precision than in the subsequent work. Consequently, Figures 13, 14, and 15, which correspond to Condition 1, show quite a scatter of points. With the existence of such a scatter it was quite difficult to fair a curve through the points. The general trend of the curve seems obvious but the reported value of the slope might have been better. It is significant that similar runs for the lower speed coefficients contained much less scatter, which may be partly due to the true effect of speed and partly due to the increased familiarity with operating techniques as the testing progressed. It is regrettable that sufficient time was not available in which to re-test Condition 1 in the hope of better agreement with previously reported static stability derivatives for this condition.

During the entire testing program the yaw scale could be read only to the nearest 0.1 of the yaw angle. For Condition 1, a change in 0.1 of the yaw angle meant a change in the dimensionless yawing moment of .005, which, for the scale used, made a certain amount of scatter almost inevitable.

As pointed out previously, the continued horizontal displacement of the axis was due to difficulty in resetting zero yaw when changing springs. The vertically displaced axis which occurred in only one case was in all probability due to excessive play in the pivot support.

The validity of considering slopes for front and rear pivots at the fixed trim indicated for free-to-trim at zero yaw seems adequately illustrated by the agreement between computed and calculated values. Therefore, since only small angles of yaw were considered, the differences in the slopes for fixed trim at zero yaw were satisfactory measures of the slope of the transverse force at zero yaw. The slope of the transverse force vs. yaw angle was considered linear for the range of small yaw angles. The only satisfactory measure of the moment curve vs. yaw angle slope was obtained at zero yaw angle for the free-to-trim condition. The moment curve is evidently much more sensitive to trim angle than the transverse force curve.

In the early stages of the testing schedule it was felt that water interference with the tail cone might possibly be contributing to the scatter of points as observed in Figure 13. In order to check this effect, a check test with spray or breaker strips was made. Subsequent to the installation of these, data were discovered in a previous test for tail cone spray strips on a similar model. For the speed ranges considered, it was found that previous results did not contribute anything to the data

and since nothing was known conerning the best position for the tail strips, they were removed for subsequent testing at the two lower speed coefficients. The addition of the strips, it was felt, might have produced more uniform results.

The operation of the apparatus depends on the fact that the model and retaining springs form a stable system. Pierson (Reference 2) has suggested a method for trying to obtain points on the moment curve which normally would be impossible to get due to the stiffness of the spring. Figure 4 shows a typical yawing moment curve with the equilibrium position that the model will assume depending on the angle of standing yaw. The process involves pushing the model while in motion to force it to assume an equilibrium position other than what it would normally take. The process has been used to advantage on unstable hulls. In the case of the lower speed coefficients where the hull has three stable branches, this method was tried but without success.

The type of mechanism used to hold the hull at fixed trim was probably not as good as it might have been. The friction lock was too close to the pivot point of suspension. It was originally designed for lock on the front pivots only, until it was decided that the moment curves were best compared at the exact same angle of trim and therefore must lock on the back pivots too. The friction lock was attached to a bracket on the midship section and to a projection on the pivot support rod. When the model was set at an angle of trim, it is believed that because

the apparatus was not correctly aligned, a slight angle of heel and angle of yaw were set into the model. This can account for the difficulty of zero yaw and zero heel for fixed trims.

The choice of the model used during the testing position of this investigation was dictated from consideration of the wealth of previous test data already in existence for this particular model. Dueto personal inexperience with model testing technique, it was felt that use of such a model would provide many desirable check points. Unfortunately, the existence of so much available test data also meant that the model had received an excessive amount of use and could not be put into very good shape. It would, in all probability, have been much better had a newer model been immediately available.

CONCLUDING REMARKS

The methods described in this report permit the lateral forces acting on a forebody and afterbody to be estimated by equations (14) and (15) on the basis of the yawing moment and lateral force obtained in a yaw test in a straight towing tank. The rotary derivatives are then obtained from equations (20) and (21).

Alternatively, it is possible to base the calculations on the angle of trim obtained from a simple zero yaw test, and to make an estimate of the wetted areas and centers of pressures on the basis of the empirical formulae of Reference 10.

Figure 22 shows a graphical comparison of computed and test values of the static stability derivatives. It will be observed that the greatest divergence between tested and computed values of $\partial N'/\partial \beta$ occurs at the lowest value of speed coefficient used. The reason for this is not too clear. Down to $C_V = 2.31$, the hull has been rapidly becoming more stable with decreasing C_V. From the composite static stability chart of Reference 2, it may be seen that with a further decrease in C_V from a value of 2.31, the hull becomes unstable. This indicates that values of C_V from 2.3 to 2.4 lie in a transition region. It is possible, therefore, that there is some change in the transverse slope of the wave in this region which affects the afterbody. Such a change in the wave form would not be predicted by the extrapolation used in computing the lateral force due to the trans-

verse wave.

The procedure developed in the analysis section of this report for predicting the static stability derivatives shows a reasonable agreement for the speed range considered for hulls of conventional design with results obtained from standard yawing tests. Unfortunately, it was not possible to check agreement in regard to the rotary derivatives since no experimental information exists concerning these.

It is believed that a more complete comparison between tested and computed values of the derivatives was not possible and a closer agreement was not obtained because of the following conditions:

a. Absence of data on the longitudinal wave profile at low values of C_V .

b. Insufficiently complete and accurate data on the transverse wave profiles.

c. Absence of sufficient experimental data on the rotary stability derivatives.

It is suggested that steps be taken to correct the above deficiencies, and that the same type of investigation as described herein might profitably be applied to other types of hulls and at a wider range of speed coefficients.

REFERENCES

1. Locke, F.W.S., Jr. Some Yawing Tests of a 1/30-scale Model of the Hull of the XPB2M-1 Flying Boat. Wartime Report ARR 3G06, NACA, Washington, D.C.

2. Pierson, J.D. Directional Stability of Flying Boat Hulls During Taxiing. Journal of the Aeronautical Sciences, July 1944, v. 11, p. 3.

3. Flickinger, P. Experimental Towing Tank Classified Report No. 398. Stevens Institute of Technology, Hoboken, N.J. October 1950.

4. Libbey, L.B. The Effectiveness of Water Rudders on Flying Boats. Thesis, Stevens Institute of Technology, Hoboken, N.J., 1950.

5. Beck, P.E. Investigation of Hydroflaps for Steering Seaplanes. Thesis, Stevens Institute of Technology, Hoboken, N.J., 1951.

6. Korvin-Kroukovsky, B.V. Hydrodynamic Design of Seaplanes. Unedited Class Notes (FD 215), Stevens Institute of Technology, Hoboken, N.J., 1950. (Unpublished)

7. Wittke, J.P. Experimental Towing Tank Classifed Report No. 400, Stevens Institute of Technology, Hoboken, N.J. February 1951.

8. Davidson, K.S.M. and Schiff, L.I. Turning and Course-Keeping Qualities. Transactions of the Society of Naval Architects and Marine Engineers, 1946.

9. Locke, F.W.S. Experimental Towing Tank Classified Report No. 198. Stevens Institute of Technology, Hoboken, N.J. December, 1942.

10. Savitsky, D. Wetted Length and Center of Pressure of Vee-step Planing Surfaces. Sherman M. Fairchild Fund Paper No. FF-6, Institute of the Aeronautical Sciences, September 1951. (Experimental Towing Tank Report No. 378, Stevens Institute of Technology, Hoboken, N.J.)

11. Korvin-Kroukovsky, B.V., Savitsky, D., and Lehman, W.F. Wave Profile of a Vee-Planing Surface Including Test Data on a 30-degree Deadrise Surface. Sherman M. Fairchild Fund Paper No. 229, Institute of Aeronautical Sciences, April 1949. (Experimental Towing Tank Report

No. 339, Stevens Institute of Technology, Hoboken, N.J.)

12. Korvin-Kroukovsky, B.V., Savitsky, D. and Lehman, W.F. Wave Contours in the Wake of a 20-degree Deadrise Planing Surface. Sherman M. Fairchild Fund Paper No. 168, Institute of Aeronautical Sciences, June 1948. (Experimental Towing Tank Report No. 337, Stevens Institute of Technology, Hoboken, N.J.)

13. Locke, F.W.S. Jr. Handbook of Instructions for the Seaplane Department, 2nd Edition, Experimental Towing Tank, Stevens Institute of Technology, Hoboken, N.J., July 15, 1943.

14. Locke, F.W.S., Jr. A Study of Porpoising Characteristics of a 1/22-scale Model of the PBM-3 Flying Boat. Experimental Towing Tank Report No. 187, Stevens Institute of Technology, Hoboken, N.J., June 20, 1942.

APPENDIX I

It is desired to obtain the equations of motion for a body moving in a nonviscous and incompressible fluid. From any standard text on vector analysis, one finds the following expression for the linear momentum and the angular momentum:

$$M\left(\frac{d\vec{V}}{dt}\right)_{\substack{\text{fixed}\\\text{system}}} = M\left(\frac{d\vec{V}}{dt}\right)_{\substack{\text{moving}\\\text{system}}} + \vec{\Omega} \times M\vec{V}$$

$$\left(\frac{d\vec{H}}{dt}\right)_{\substack{\text{fixed}\\\text{system}}} = \left(\frac{d\vec{H}}{dt}\right)_{\substack{\text{moving}\\\text{system}}} + \vec{\Omega} \times \vec{H}$$

where the vectors have the value

$$\vec{V} = ui + vj + wk$$

$$\vec{\Omega} = pi + qj + rk$$

$$\vec{H} = h_x i + h_y j + h_z k \quad .$$

Evaluating the vector product by the matrix, equating like components, and applying Newton's law to the coordinate axes fixed in space gives

$$\vec{\Omega} \times \vec{MV} = \begin{vmatrix} i & j & k \\ p & q & r \\ m_1'u & m_2'v & m_3'w \end{vmatrix}$$

$$F_1 = m_1'\dot{u} - m_2'vr + m_3'wq = X$$

$$F_2 = m_2'\dot{v} + m_1'ur - m_3'wp = Y$$

$$F_3 = m_3'\dot{w} + m_2'vp - m_1'uq = Z$$

$$M\left(\frac{d\vec{V}}{dt}\right)_{\substack{\text{fixed}\\ \text{system}}} = \vec{F} \quad \text{(resultant force)}$$

$$\vec{F} = F_1 i + F_2 j + F_3 k$$

$$\vec{\Omega} \times \vec{H} = \begin{vmatrix} i & j & k \\ p & q & r \\ h_x & h_y & h_z \end{vmatrix}$$

$$= i(h_z q - r h_y) + j(r h_x - p h_z) + k(p h_y - q h_x)$$

$$\left(\frac{d\vec{H}}{dt}\right)_{\substack{\text{fixed}\\ \text{system}}} = \vec{G} \quad \text{(resultant torque)}$$

$$\vec{G} = G_1 i + G_2 j + G_3 k$$

$$G_1 = \dot{h}_x - r h_y + q h_z = L$$
$$G_2 = \dot{h}_y + r h_x - p h_z = M$$
$$G_3 = \dot{h}_z + p h_y - q h_x = N$$

The forces F are the externally applied forces acting in a Newtonian frame of reference, the components of which are found by equating like components of the original equations. From geometrical considerations, one considers an element of mass "dm" and determines the contribution of this mass to the angular momentum about the three coordinate axes. It is shown that

$$h_x = Ap - Fq - Er$$
$$h_y = -Fp + Bq - Dr$$

$$h_z = - Ep - Dq + Cr$$

where

$$A = I_x \qquad D = I_{yz}$$

$$B = I_y \qquad E = I_{xz}$$

$$C = I_z \qquad F = I_{xy}$$

which for a symmetrical body taken along the principal axis, the products of inertia will vanish, leaving

$$h_x = Ap$$

$$h_y = Bq - Dr$$

$$h_z = - Dq + Cr \quad .$$

The problem to be investigated is concerned only with yaw; therefore, it is supposed that the motion in the horizontal plane may be considered separately. This leads to the more simple form of the equations of motion since roll and pitch and heave are made zero. The final equations desired, then, are as follows:

$$\left.\begin{aligned} m_1'\dot{u} - m_2'vr &= X \\ m_2'\dot{v} + m_1'ur &= Y \\ I_z\dot{r} &= N \end{aligned}\right\} \qquad \text{(I-1)}$$

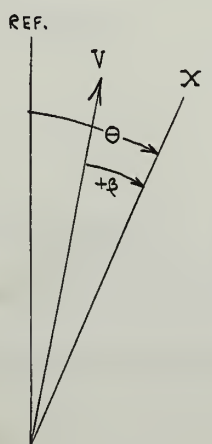

In order to solve these equations, one makes several transformations by putting the various terms into dimensionless parameters. With reference to the accompanying figure, the following substitutions are made and put into the original equations:

$$u = V \cos \beta$$

$$v = - V \sin \beta$$

$$\dot{u} = \dot{V} \cos \beta - V \sin \beta \, \dot{\beta}$$

$$\dot{v} = - \left(\dot{V} \sin \beta + V \dot{\beta} \cos \beta \right)$$

$$r = \frac{d\theta}{dt} = \dot{\theta}$$

$$\dot{r} = \ddot{\theta}$$

$$\left.\begin{aligned} m_1' \dot{V} \cos \beta - m_1' V \dot{\beta} \sin \beta + m_2' V \dot{\theta} \sin \beta &= X \\ -m_2' \dot{V} \sin \beta - m_2' V \dot{\beta} \cos \beta + m_1' V \dot{\theta} \cos \beta &= Y \\ I_z \ddot{\theta} &= N \end{aligned}\right\} \quad \text{(I-2)}$$

When the original equations were developed, the mass was merely referred to in three different directions coinciding with the coordinate axes. Now, with the aid of the "ellipsoid approximation," the mass in the X and Y direction have the following standard seaplane notation:

$$m_1' = m + m_o k_1$$

$$m_2' = m + m_o k_2$$

where m is the mass of the seaplane, m_o is the mass of the displaced fluid, and k_1 is the virtual mass coefficient in the X direction. The following dimensionless substitutions are

then made:

$$X' = \frac{X}{\frac{\rho}{2}V^2b^2} \qquad m_1 = \frac{m + m_o k_1}{\frac{\rho}{2}b^3}$$

$$Y' = \frac{Y}{\frac{\rho}{2}V^2b^2} \qquad m_2 = \frac{m + m_o k_2}{\frac{\rho}{2}b^3}$$

$$N' = \frac{N}{\frac{\rho}{2}V^2b^3} \qquad n = \frac{I_z + k' I_{z_o}}{\frac{\rho}{2}b^5}$$

$$\frac{m_1 b\dot{V}\cos\beta}{V^2} - \frac{m_1 Vb\dot{\beta}\sin\beta}{V^2} + \frac{m_2 Vb\dot{\theta}\sin\beta}{V^2} = X' \quad .$$

A quantity s is introduced which is a distance defined as:

$$s = \frac{Vt}{b} \quad ,$$

and therefore all derivatives may be replaced in terms of this dimensionless parameter as follows:

$$\frac{d}{dt} = \frac{d}{ds}\frac{ds}{dt}$$

$$\frac{d}{dt} = \frac{V}{b}\frac{d}{ds}$$

$$\frac{d(\ )}{ds} = (\ )' = \frac{b}{V}\frac{d(\ )}{dt}$$

$$\beta' = \frac{\dot{\beta}b}{V} \quad ; \quad V' = \frac{\dot{V}b}{V} \quad ; \quad \theta' = \frac{\dot{\theta}b}{V} = r'$$

$$\dot{r} = \frac{dr'}{dt}\frac{V}{b} + \frac{r'}{b}\frac{dV}{dt}$$

$$= r''\frac{V^2}{b^2} + \frac{VV'}{b^2}$$

Substituting these into equations (I-2) and limiting the discussion to small values of β, it follows that the three equa-

tions take the following form:

$$X' = \frac{m_1 V'}{V} - m_1 V\beta'\beta + m_2 r'\beta$$

$$Y' = \frac{-m_2 V'}{V}\beta - m_2\beta' + m_1 r'$$

$$N' = nr'' + \frac{r'V'n}{V}$$

For steady course, it is noted that V' is at least first order in β and r' since X' is zero for steady course, and further that V' is at least second order in Y' and N' so that V' may be made equal to zero. Since the motion under consideration is concerned only with the horizontal plane, the force Y' and the moment N' may be considered to be functions of β and r'. Expanding into a Taylor series and neglecting higher order terms gives

$$N' = \frac{\partial N'}{\partial \beta}\beta + \frac{\partial N'}{\partial r'} r'$$

$$= N'_\beta \beta + N'_r r'$$

$$Y' = \frac{\partial Y'}{\partial r'} r' + \frac{\partial Y'}{\partial \beta}\beta$$

$$= Y'_{r'} r' + Y'_\beta \beta \quad .$$

For initial values taken as zero, changes are small and assumed to remain in the linear region.

By substituting these expressions, the following differential equations are obtained:

$$m_2\beta' + Y'_\beta \beta - r'(m_1 - Y'_{r'}) = 0$$

$$nr'' - N'_{r'} r' - N'_\beta \beta = 0 \quad .$$

Using operator notation, two simultaneous equations are solved; the solution is obtained from the quadratic formula. The solution represents the roots of the quadratic and is a solution to the differential equations.

$$D = \frac{d}{ds}$$

$$\beta(m_2 D + Y'_\beta) - r'(m_1 - Y'_{r'}) = 0$$
$$r'(nD - N'_{r'}) - N'_\beta \beta = 0$$

$$\frac{m_1 - Y'_{r'}}{m_2 D + Y'_\beta} = \frac{(nD - N'_{r'})}{N'_\beta}$$

$$m_2 n D^2 + D(nY'_\beta - m_2 N'_{r'}) + Y'_\beta N'_{r'} - N'_\beta (m_1 - Y'_{r'}) = 0$$

$$D = \sigma_{1,2}$$

$$= \frac{-(nY'_\beta - m_2 N'_{r'})}{2m_2 n}$$

$$\pm \frac{\left\{(nY'_\beta - m_2 N'_{r'})^2 + 4m_2 n \left[Y'_\beta N'_{r'} + N'_\beta (m_1 - Y'_{r'})\right]\right\}^{1/2}}{2m_2 n}$$

APPENDIX II

Mathematical Calculations for Condition 2 of Table IV

For Condition 2 it was found that the speed coefficient was much too low for laying out the longitudinal wave profile as shown in Reference 8. The process then was one of trial and error in order to determine forces and distances as shown in the mathematical analysis section of this investigation. For the lower speed coefficients it was impossible to get the added increase in afterbody load that was necessary since the load carried by the forebody decreased as the speed coefficient decreased and therefore the afterbody load must be increasing.

Forebody Conditions

$\tau = 11.2$

$C_V = 2.46$

$(C_V)^2 = 6.04$

$C_\Delta = 0.6$

$$C_{L_\beta} = \frac{2(.6)}{6.04} = .1985$$

$$C_{L_\beta} = .262 - .143(.448) = .262 - .064$$
$$= .198$$

$$C_{L_o} = .262$$

$$\frac{C_{L_o}}{\tau^{1.1}} = .01832$$
$$= .0120(1.51)^{\frac{1}{2}} + .001572(1.52)^2 = .01476 + .00357$$
$$= .01832$$

$\therefore \lambda = 1.51$

$\Delta = .6(62.3)(1000) = 37,400$

$(\Delta)_F = \frac{37,400}{\cos 11.2^o} = 38,100$

$$C_P = .75 - \frac{1}{3.06\left(\frac{6.04}{1.855}\right) + 2.42} = .669$$

$P = .669(15.1) = 10.11$

$\ell_1 = 10.11 - 3.67 = 6.44$

Afterbody

$(\Delta)_A = 49,750 - 37,400 = 12,350$

For b = 6.8,

$$C_{L_\beta} = \frac{2 \times 12,350}{1.937(1935)(46)} = .143$$

$C_{L_\beta} = .216 - .182(.399)$

$= .1434$

$C_{L_o} = .216$

For $\forall = 10.2$,

$$\frac{C_{L_o}}{\forall^{1.1}} = .01687$$

$= .012(1.47)^{\frac{1}{2}} + .001068(1.47)^2 = .01457 + .00230$

$= .01687$

$\therefore \lambda = 1.47$

$$C_P = .75 - \frac{1}{15.55 + 2.42} = .75 - .056 = .694$$

$\ell_m = 1.47(6.8) = 10$ ft. $= 120$ in.

$\ell_k = 2\ell_m = 240$ in.

$P = .694(10) = 6.94$ ft. $= 83.2$ in.

$$\tan \gamma = \frac{1}{\frac{2}{\pi}\frac{.531}{.1796}} = .532$$

$\gamma = 28^{\circ}$

$\ell_2 = 13.83 + 3.67$ (Figure 9)

$= 17.50$ ft.

Forebody Frictional Resistance

$$(Re)_m = \frac{9.43\left(\frac{15.1}{22}\right)}{1.08 \times 10^{-5}} = 5.99 \times 10^5$$

$$(C_F)_m = \frac{.0074}{1.431} = .00516$$

$$(C_R)_m = .00516(1.51)\left(\frac{1}{.927}\right) = .00842$$

$$R = .00842\left(\frac{1.937}{2}\right)(1935)(100)$$

$= 1578$ lb.

Afterbody Frictional Resistance

$$(Re)_m = \frac{9.43\left(\frac{10.0}{22}\right)}{1.08 \times 10^{-5}} = 3.97 \times 10^{-5}$$

$$(C_F)_m = \frac{.0074}{1.317} = .00562$$

$$(C_R)_m = .00562(1.47)\left(\frac{1}{.883}\right) = .00937$$

$$R = .00937\left(\frac{1.937}{2}\right)(1935)(46)$$

$= 806$ lb.

Total $R = (1578 + 806)1.25 = 2980$ lb.

Moments about C.G.

$38,100(6.44) = 10(2,980) + 17.50(12,350)$

$245,500 = 29,800 + 216,500$

$\cong 246,300$.

Forebody Transverse Force (consult Figure 11(b))

$\Delta \tau = .374$ (for 1° yaw)

$$(\Delta)_R = 19.050 \left(\frac{11.2 + .374}{11.2}\right) = 19,678$$

$$(\Delta)_L = 19,050 \left(\frac{11.2 - .374}{11.2}\right) = 18,314$$

$\tan 22^\circ(19,678) = 7.950$

$\tan 22^\circ(18,314) = \underline{7,399}$

Net Force = 551

Afterbody Transverse Force

$$(\Delta)_R = 6,175 \left(\frac{10.2 + .47}{10.2}\right) = 6.459$$

$$(\Delta)_L = 6,175 \left(\frac{10.2 - .47}{10.2}\right) = 5,890$$

$\tan 28^\circ$ (6,459) = 3,436

$\tan 28^\circ$ (5,890) = 3,134

Net Force = 302 lb.

Additional Afterbody Transverse Force (Figure 32 (Reference 7))

distance from $\mathbb{C}$ = .3

slope 1 beam = 19°

slope 2 beams = 16.8
Average = 17.9

$\tan 17.9^\circ = .323$

center of pressure travel = $\frac{17.50}{57.3} = .305$

vertical distance = $(.305)(.323) = .0985$

total = $2(.0985) = .1972$

wave slope = $\frac{.1972}{6.8} = .029$

added force = $(.029)(12{,}350) = 3.58$ lb.

Correction:

$$358\left(\frac{1}{\frac{3.71}{2.46}.9}\right)\quad\frac{22}{20} = 290 \text{ lb.}$$

$$\frac{\partial Y'}{\partial \beta} = \frac{2(551 + 592)}{1.937(1935)(100)}$$

$= .0061$/degree

$= .349$/radian

$$\frac{\partial N'}{\partial \beta} = \frac{2\left[551(6.44) - 592(17.50)\right]}{1.937(1935)(1000)}$$

$= - .00364$/degree

$= - .208$/radian

Mathematical Calculations for Condition 3 of Table IV

Forebody Conditions:

$\tau = 10.5^\circ$

$C_V = 2.34$

$(C_V)^2 = 5.47$

$C_\Delta = 0.56$

$C_{L_\beta} = \frac{2(.56)}{5.47} = .205$

$$C_{L_\beta} = .270 - .143(.456)$$

$$= .205$$

$$C_{L_o} = .270$$

$$\frac{C_{L_o}}{\tau^{1.1}} = .0203$$

$$= .0120(1.293) + .001737(2.78)$$

$$= .01551 + .00483$$

$$= .02034$$

$\therefore \lambda = 1.67$

$$\Delta = .56(62.3)(1000) = 34,900$$

$$(\Delta)_F = \frac{34,900}{\cos 10.5^o} = 35,500$$

$$C_P = .75 - \frac{1}{7.77 + 2.42}$$

$$= .652$$

$$P = .652(16.7) = 10.9$$

$$\ell_1 = 10.9 - 3.67 = 7.23$$

Afterbody Conditions

$$(\Delta)_A = 49,750 - 34,900 = 14,850$$

For b = 7.5

$$C_{L_\beta} = \frac{2 \times 14,850}{1.937(1720)(56)} = .1595$$

$$C_{L_\beta} = .235 - .182(.419)$$

$$= .235 - .076$$

$$= .159$$

$$C_{L_o} = .235$$

For $\nabla = 10.3$

$$\frac{C_{L_o}}{\nabla^{1.1}} = .01805$$

$$= .0120(1.246) + .001296(2.4)$$

$$= .01494 + .00311$$

$$= .01805$$

$$\lambda = 1.55$$

$$\ell_m = 1.55(7.5)$$

$$= 11.62 \text{ ft.} = 139.6 \text{ in.}$$

$$\ell_k = 2\ell_m = 279.2 \text{ in.}$$

$$C_P = .75 - \frac{1}{11.62 + 2.42} = .75 - .071 = .679$$

$$P = .679(11.62) = 7.9 \text{ ft.} = 94.7 \text{ in.}$$

$$\ell_2 = 11.59 + 3.67 = 15.26$$

Forebody Frictional Resistance

$$(Re)_m = \frac{8.988 \left(\frac{16.7}{22}\right)}{1.08 \times 10^{-5}} = 6.32 \times 10^5$$

$$(C_F)_m = \frac{.0074}{1.446} = .00512$$

$$(C_R)_m = .00512(1.67) \frac{1}{.927} = .00922$$

$$R = .00922 \left(\frac{1.937}{2}\right) (1720)(100)$$

$$= 1535 \text{ lb.}$$

Afterbody Frictional Resistance

$$(Re)_m = \frac{8.988 \left(\frac{11.62}{22}\right)}{1.08 \times 10^{-5}} = 4.40 \times 10^5$$

$$(C_F)_m = \frac{.0074}{1.345} = .0055$$

$$(C_R)_m = .0055(1.55)\left(\frac{1}{.883}\right)$$

$$= .00965$$

$$R = .00965\left(\frac{1.937}{2}\right)(1720)(56)$$

$$= 900 \text{ lb.}$$

Total R = 1.25(1535 + 900) = 3,050

Moments About C.G.

35,500(7.23) = 14,850(15.26) + 10(3,050)

257,000 = 226,000 + 30,500

$\cong$ 256,500

Forebody Transverse Force

$$(\Delta)_R = 17,750\left(\frac{10.5 + .374}{10.5}\right) = 18,382$$

$$(\Delta)_L = 17,750\left(\frac{10.5 - .374}{10.5}\right) = 17,108$$

tan 22° (18,382) = 7,426

tan 22° (17,108) = 6,912

Net Force = 514 lb.

Afterbody Transverse Force

$$(\Delta)_R = 7,425\left(\frac{10.3 + .47}{10.3}\right) = 7,764$$

$$(\Delta)_L = 7{,}425 \left(\frac{10.3 - .47}{10.3} \right) = 7{,}085$$

tan 28 (7,764) = 4,130

tan 28 (7,085) = 3,769

Net Force = 361 lb.

distance from ℄ = .4

slope 1 beam = 24°

slope 2 beams = 20°

Average = 22°

tan 22° = .404

center of pressure of travel = $\frac{15.26}{57.3}$ = .266

vertical distance = (.404)(.266) = .1076

total = 2(.1076) = .2152

wave slope = $\frac{.2152}{7.5}$ = .0287

added force = (.0287) 14,850 = 426

Correction:

$$426 \left(\frac{1}{\frac{3.71}{2.34}(.9)} \right) \frac{22}{20} = 328$$

$$\frac{\partial Y'}{\partial \beta} = \frac{2(514 + 689)}{1.937(1720)(100)}$$

= .00722/degree

= .414/radian

$$\frac{\partial N'}{\partial \beta} = \frac{2\left[514(7.23) - 689(15.26)\right]}{1.937(1720)(1000)}$$

= -.00408/degree

= -.234/radian

TABLE I

MODEL PARTICULARS

Stevens Model No.	406
Scale	1/22
Beam at main step, in.	5.45
Forebody length, in.	18.30
Afterbody length, in.	14.93
Angle between forebody keel and baseline, deg.	0
Angle between afterbody keel and baseline, deg.	7.5
Deadrise at keel and main step (average)	22
Deadrise on afterbody (average)	28
Height of main step at keel, in.	.27
C.G. forward of main step, in.	2.0
C.G. above baseline, in.	6.0

TABLE II

AFTERBODY DIMENSIONS

Station, Inches from Step	Keel Height from Baseline Extension, in.	Chine Height from Baseline Extension, in.	b/2, Half Beam, in.	β, Deadrise Angle, deg.
0	6.00	27.1	57.6	26
71	14.96	41.4	54.0	26
154	25.5	49.6	43.3	28
245	37.4	49.5	26.0	28
314	46.4	50.0	6.60	28

TABLE III

LONGITUDINAL WAVE PROFILE

(X and H are Fractions of Maximum Beam)

X	1	2	3	4	5	6
H_o	.143	.452	.810	1.17	1.40	1.52
H_λ	.0316	.0632	.0948	.1265	.158	.1895
H	.1746	.5152	.9048	1.2965	1.558	1.7095
H, in.	20.85	61.8	108.5	155.5	187	205
H, in., Reduced 90%	18.8	55.6				

Conditions: $C_V = 2.62$; $C_\Delta = 0.8$; $\tau = 12.6^\circ$

TABLE IV

TESTING DATA

Condition	C_V	V_m, ft./sec.	Speed No.	τ, deg.	$\frac{\rho}{2} V^2 b^3$	C_Δ	V_s, ft./sec.	C_M	V^2
1	2.63	10.065	H_1-22	12.6	9.16	0.8	47.1	0	2210
2	2.46	9.43	H_2-10	11.0	8.58	0.8	44.1	0	1935
3	2.34	8.988	H_1-19	10.5	7.31	0.8	41.6	0	1720

TABLE V

PLANING HYDRODYNAMIC CHARACTERISTICS

FOR THREE SPEED COEFFICIENTS

C_V	C_Δ	Δ_F, lb.	λ_F	λ_A	τ_F, deg.	τ_A, deg.	R_F, lb.	R_A, lb.	Total R + 25%	γ, deg.	b_A, ft.	Δ_A, lb.	ℓ_1, ft.	ℓ_2, ft.
2.63	.648	40,300	1.25	1.42	12.6	9.6	1530	670	2880	$26^\circ 20'$	5.83	8,950	4.99	19.87
2.46	.60	37,400	1.51	1.47	11.2	10.2	1578	806	2980	28	6.8	12,350	6.44	17.50
2.34	.560	34,900	1.67	1.55	10.5	10.3	1535	900	3050	$28^\circ 20'$	7.5	14,850	7.23	15.26

TABLE VI

FREE-TO-TRIM

C_V = 2.63
C_Δ = 0.8
Tail Cone Spray Strips

Δ_o = 4.24
$+^o$ = .42
Δ = 4.66(lb.)

Run No.	Ψ(Still), deg.	Ψ(Moving), deg.	$\Delta\Psi$	N, in.-lb.	N, ft.-lb.	N'	Ψ, deg.	ζ, deg.
1	6.0P	5.3P	+.7	+3.88	+.323	+.0352	5.3P	15.0
2	5.0P	4.8P	+.2	+1.11	+.0925	+.01007	4.8P	14.5
3	4.5P	4.4P	+.1	+ .554	+.0461	+.00502	4.4P	13.8
4	4.1P	3.8P	+.3	+1.66	+.138	+.015	3.8P	13.5
5	3.5P	3.3P	+.2	+1.11	+.0925	+.01007	3.3P	13.0
6	3.0P	2.8P	+.2	+1.11	+.0925	+.01007	2.8P	13.0
7	2.6P	2.5P	+.1	+ .554	+.0461	+.00502	2.5P	12.8
8	2.0P	1.8P	+.2	+1.11	+.0925	+.01007	1.8P	12.8
9	1.5P	1.3P	+.2	+1.11	+.0925	+.01007	1.3P	12.7
10	1.0P	.9P	+.1	+ .554	+.0461	+.00502	.9P	12.9
11	.5P	.4P	+.1	+ .554	+.0461	+.00502	.4P	12.7
12	.6S	.5S	-.1	- .554	-.0461	-.00502	.5S	12.8
13	1.0S	.9S	-.1	- .554	-.0461	-.00502	.9S	12.6
14	1.5S	1.4S	-.1	- .554	-.0461	-.00502	1.4S	13.0
15	1.9S	2.1S	+.2	+1.11	+.0925	+.01007	2.1S	13.3
16	2.5S	2.4S	-.1	- .554	-.0461	-.00502	2.4S	13.0
17	3.0S	2.9S	-.1	- .554	-.0461	-.00502	2.9S	13.4
18	3.5S	3.6S	+.1	+ .554	+.0461	+.00502	3.6S	13.6
19	4.0S	3.8S	-.2	-1.11	-.0925	-.01007	3.8S	13.8
20	4.5S	4.3S	-.2	-1.11	-.0925	-.01007	4.3S	14.2
21	5.0S	4.8S	-.2	-1.11	-.0925	-.01007	4.8S	14.6
22	6.0S	6.4S	+.4	+2.22	+.185	+.0201	6.4S	15.0

TABLE VII

FIXED TRIM; FRONT PIVOTS

$\tau = 12.6^{\circ}$
$C_V = 2.63$
$C_\Delta = 0.8$
Tail Cone Spray Strips

$\Delta_{+^{\circ}} = 4.24$
$\Delta_{+^{\circ}} = .42$
$\Delta = 4.66$(lb.)

Run No.	γ(Still), deg.	γ(Moving), deg.	$\Delta\gamma$	N, in.-lb.	N, ft.-lb.	N'	γ, deg.
1	5.0S	6.4S	+1.4	+7.76	+.646	+.0704	6.4S
2	4.5S	5.1S	+ .6	+3.32	+.276	+.0301	5.1S
3	3.9S	4.4S	+ .5	+2.77	+.231	+.0251	4.4S
4	3.3S	2.6S	- .5	-2.77	-.231	-.0251	2.6S
5	2.5S	2.3S	- .2	-1.11	-.0925	-.01	2.3S
6	1.9S	1.5S	- .4	-2.22	-.185	-.0201	1.5S
7	1.3S	1.1S	- .2	-1.11	-.0925	-.01	1.1S
8	.5S	.3S	- .2	-1.11	-.0925	-.01	.3S
9	0	0	0	0	0	0	0
10	.6P	.5P	+ .1	+ .554	+.0461	+.005	.5P
11	1.1P	.9P	+ .2	+1.11	+.0925	+.01	.9P
12	1.8P	1.7P	+ .1	+ .554	+.0461	+.005	1.7P
13	2.6P	2.4P	+ .2	+1.11	+.0925	+.01	2.4P
14	3.1P	3.0P	+ .1	+ .554	+.0461	+.005	3.0P
15	3.6P	3.3P	+ .3	+1.66	+.138	+.0151	3.3P
16	4.1P	3.8P	+ .3	+1.66	+.138	+.0151	3.8P
17	4.7P	4.6P	+ .1	+ .554	+.0461	+.005	4.6P
18	5.5P	5.1P	+ .4	+2.22	+.185	+.0201	5.1P

TABLE VIII

FIXED TRIM; BACK PIVOTS

$\tau = 12.6^{\circ}$
$C_V = 2.63$
$C_{\Delta} = 0.8$
Tail Cone Spray Strips

$\Delta_o = 4.24$
$+^{\circ} = .42$
$\Delta = 4.66$(lb.)

Run No.	γ(Still), deg.	γ(Moving), deg.	$\Delta\gamma$	N, in.-lb.	N, ft.-lb.	N'	γ, deg.
1	4.0S	4.8S	+ .8	+4.43	+.369	+.0401	4.8S
2	2.8S	2.7S	- .1	- .554	-.0461	-.005	2.7S
3	2.4S	2.4S	0	0	0	0	2.4S
4	2.0S	2.2S	+ .2	+1.11	+.0925	+.01	2.2S
5	1.5S	1.4S	- .1	- .554	-.0461	-.005	1.4S
6	1.0S	.8S	- .2	-1.11	-.0925	-.01	.8S
7	.5S	.4S	- .1	- .554	-.0461	-.005	.4S
8	.6P	.4P	+ .2	+1.11	+.0925	+.01	.4P
9	1.1P	.9P	+ .2	+1.11	+.0925	+.01	.9P
10	1.6P	1.5P	+ .1	+ .554	+.0461	+.005	1.5P
11	2.0P	2.0P	0	0	0	0	2.0P
12	2.6P	2.4P	+ .2	+1.11	+.0925	+.01	2.4P
13	3.1P	2.8P	+ .3	+1.66	+.138	+.0151	2.8P
14	3.6P	3.4P	+ .2	+1.11	+.0925	+.01	3.4P
15	4.1P	3.9P	+ .2	+1.11	+.0925	+.01	3.9P
16	4.5P	4.4P	+ .1	+ .554	+.0461	+.005	4.4P
17	5.1P	5.0P	+ .1	+ .554	+.0461	+.005	5.0P
18	.5S	.6S	+ .1	+ .554	+.0461	+.005	.6S
19	1.0S	.8S	- .2	-1.11	-.0925	-.01	.8S
20	1.5S	1.4S	- .1	- .554	-.0461	-.005	1.4S
21	2.0S	1.9S	- .1	- .554	-.0461	-.005	1.9S
22	2.5S	2.3S	- .2	-1.11	-.0925	-.01	2.3S
23	2.9S	2.8S	- .1	- .554	-.0461	-.005	2.8S
24	3.4S	3.3S	- .1	- .554	-.0461	-.005	3.3S
25	4.0S	3.8S	- .2	-1.11	-.0925	-.01	3.8S
26	5.0S	6.0S	+1.0	+5.54	+.461	+.05	6.0S

TABLE IX

FREE-TO-TRIM

C_V = 2.46
C_Δ = 0.8
No Spray Strips

Δ_o = 4.36
$+^o$ = .30
Δ = 4.66(lb.)

Run No.	Ψ(Still), deg.	Ψ(Moving), deg.	$\Delta\Psi$	N, in.-lb.	N, ft.-lb.	N'	Ψ deg.	ζ deg.
1	.5S	.4S	- .1	- .211	-.0176	-.00205	.4S	11.2
2	1.0S	.9S	- .1	- .211	-.0176	-.00205	.9S	
3	1.5S	1.4S	- .1	- .211	-.0176	-.00205	1.4S	
4	2.0S	1.7S	- .3	- .633	-.0527	-.00614	1.7S	
5	2.5S	2.1S	- .4	- .844	-.0703	-.0082	2.1S	12.0
6	2.9S	2.4S	- .5	-1.055	-.088	-.01025	2.4S	12.2
7	3.5S	2.7S	- .8	-1.688	-.1405	-.01637	2.7S	12.1
8	4.0S	2.8S	-1.2	-2.53	-.211	-.0246	2.8S	12.3
9	4.0S	5.3S	+2.3	+4.86	+.405	+.0471	5.3S	14.0
10	4.5S	6.5S	+2.0	+4.22	+.352	+.041	6.5S	
11	5.0S	6.7S	+1.7	+3.59	+.299	+.0348	6.7S	
12	6.0S	7.4S	+1.4	+2.59	+.216	+.0252	7.4S	15.5
13	.6S	.6S	0	0	0	0	0	11.2
14	.6P	.4P	+ .2	+ .422	+.0352	+.0041	.4P	11.3
15	1.1P	.7P	+ .4	+ .844	+.0703	+.0082	.7P	11.1
16	1.6P	1.0P	+ .6	+1.266	+.1053	+.0123	1.0P	11.5
17	2.0P	1.3P	+ .7	+1.477	+.123	+.0143	1.3P	11.6
18	2.6P	1.5P	+1.1	+2.32	+.193	+.0225	1.5P	11.6
19	3.0P	1.8P	+1.2	+2.53	+.211	+.0246	1.8P	12.0
20	4.1P	2.3P	+1.7	+3.59	+.299	+.0348	2.3P	12.2
21	5.1P	6.3P	-1.2	-2.53	-.211	-.0246	6.3P	15.0
22	6.0P	7.0P	-1.0	-2.11	-.176	-.0205	7.0P	15.6

TABLE X

FIXED TRIM; BACK PIVOTS

$\tau = 11.2^{\circ}$
$C_V = 2.46$
$C_\Delta = 0.8$
No Spray Strips

$\Delta_{+^{\circ}} = 4.36$
$\Delta_{+^{\circ}} = .30$
$\Delta = 4.66$(lb.)

Run No.	Ψ(Still), deg.	Ψ(Moving), deg.	$\Delta\Psi$	N, in.-lb.	N, ft.-lb.	N'	Ψ, deg.
1	6.1P	7.4P	-1.3	-2.74	-.228	-.0266	7.4P
2	5.1P	6.6P	-1.5	-3.16	-.264	-.0308	6.6P
3	4.5P	6.3P	-1.8	-3.8	-.317	-.0369	6.3P
4	4.0P	6.0P	-2.0	-4.22	-.352	-.041	6.0P
5	3.5P	2.3P	+1.2	+2.53	+.211	+.0246	2.3P
6	2.9P	2.1P	+ .8	+1.69	+.141	+.0164	2.1P
7	2.5P	1.6P	+ .9	+1.9	+.158	+.0184	1.6P
8	2.0P	1.5P	+ .5	+1.055	+.088	+.0103	1.5P
9	1.5P	1.3P	+ .2	+ .422	+.0352	+.0041	1.3P
10	.9P	.7P	+ .2	+ .422	+.0352	+.0041	.7P
11	.5P	.4P	+ .1	+ .211	+.0176	+.00205	.4P
12	5.9S	7.7S	+1.8	+3.8	+.317	+.0369	7.7S
13	4.9S	7.3S	+2.4	+5.06	+.421	+.049	7.3S
14	4.4S	6.8S	+2.4	+5.06	+.421	+.049	6.8S
15	3.9S	6.5S	+2.4	+5.06	+.421	+.049	6.5S
16	3.4S	6.1S	+2.7	+5.7	+.475	+.0553	6.1S
17	2.8S	5.7S	+2.9	+6.12	+.51	+.0594	5.7S
18	2.4S	2.1S	- .3	- .633	-.0527	-.00613	2.1S
19	1.9S	1.8S	- .1	- .211	-.0176	-.00205	1.8S
20	1.5S	1.4S	- .1	- .211	-.0176	-.00205	1.4S

TABLE XI

FIXED TRIM; FRONT PIVOTS

$\tau = 11.2^{\circ}$
$C_V = 2.46$
$C_\Delta = 0.8$
No Spray Strips

$\Delta_o = 4.36$
$+^{\circ} = .30$
$\Delta = 4.66$(lb.)

Run No.	ψ(Still), deg.	ψ(Moving), deg.	$\Delta\psi$	N, in.-lb.	N, ft.-lb.	N'	ψ, deg.
1	6.1P	7.3P	-1.2	-2.53	-.211	-.0246	7.3P
2	5.0P	6.6P	-1.6	-3.38	-.282	-.0328	6.6P
3	4.5P	2.6P	+1.9	+4.01	+.334	+.0389	2.6P
4	4.0P	2.5P	+1.5	+3.16	+.263	+.0306	2.5P
5	3.5P	2.4P	+1.1	+2.32	+.193	+.0225	2.4P
6	3.0P	2.2P	+ .8	+1.69	+.141	+.0164	2.2P
7	2.0P	1.5P	+ .5	+1.057	+.088	+.0103	1.5P
8	1.0P	.9P	+ .1	+ .211	+.0176	+.00205	.9P
9	1.5P	1.3P	+ .2	+ .422	+.0352	+.0041	1.3P
10	.5P	.3P	+ .2	+ .422	+.0352	+.0041	.3P
11	6.0S	7.2S	+1.2	+2.53	+.211	+.0246	7.2S
12	5.0S	6.5S	+1.5	+3.16	+.264	+.0307	6.5S
13	4.0S	5.9S	+1.9	+4.01	+.334	+.0389	5.9S
14	3.5S	5.6S	+2.1	+4.43	+.369	+.043	5.6S
15	2.8S	5.4S	+2.6	+5.48	+.457	+.0532	5.4S
16	1.5S	1.1S	- .4	- .844	-.0703	-.0082	1.1S
17	2.0S	1.4S	- .6	-1.269	-.1057	-.0123	1.4S
18	.9S	.8S	- .1	- .211	-.0176	-.00205	.8S
19	.8S	.7S	- .1	- .211	-.0176	-.00205	.7S
20	1.2S	.9S	- .3	- .633	-.0527	-.00614	.9S

TABLE XII

FREE-TO-TRIM

C_V = 2.34
C_Δ = 0.8
No Spray Strips

Δ_o = 4.16
$+^o$ = .50
Δ = 4.66(lb.)

Run No.	ψ(Still), deg.	ψ(Moving), deg.	$\Delta\psi$	N, in.-lb.	N, ft.-lb.	N'	ψ, deg.	τ, deg.
1	1.0P	.5P	+ .5	+1.055	+.088	+.012	.5P	10.6
2	2.0P	.7P	+1.3	+2.742	+.228	+.0312	.7P	11.0
3	3.0P	1.0P	+2.0	+4.22	+.352	+.0481	1.0P	11.2
4	4.0P	2.5P	+1.5	+3.165	+.264	+.0361	2.5P	12.5
5	5.0P	5.7P	- .7	-1.477	-.123	-.0168	5.7P	15.5
6	6.0P	5.7P	+ .3	+ .633	+.0527	+.0072	5.7P	16.0
7	1.0S	.5S	- .5	-1.055	-.088	-.012	.5S	10.7
8	2.0S	1.0S	-1.0	-2.11	-.176	-.0241	1.0S	11.2
9	3.0S	2.5S	- .5	-1.055	-.088	-.012	2.5S	12.5
10	4.0S	4.5S	+ .5	+1.055	+.088	+.012	4.5S	15.5
11	5.0S	5.0S	0	0	0	0	5.0S	14.5
12	6.0S	5.4S	- .6	-1.266	-.1055	-.0144	5.4S	16.0

TABLE XIII

FIXED TRIM; BACK PIVOTS

$\tau = 10.5^{o}$
$C_V = 2.34$
$C_\Delta = 0.8$
No Spray Strips

$\Delta_o = 4.36$
$+^{o} = .30$
$\Delta = 4.66$(lb.)

Run No.	Ψ(Still), deg.	Ψ(Moving), deg.	$\Delta\Psi$	N, in.-lb.	N, ft.-lb.	N'	Ψ, deg.
1	0	0	0	0	0	0	0
2	6.1P	6.4P	- .3	-1.66	-.134	-.0183	6.4P
3	5.5P	6.0P	- .5	-2.75	-.229	-.0313	6.0P
4	5.0P	5.6P	- .6	-3.32	-.277	-.0379	5.6P
5	4.5P	5.1P	- .6	-3.32	-.277	-.0379	5.1P
6	4.0P	4.8P	- .8	-4.43	-.369	-.0505	4.8P
7	3.5P	4.3P	- .8	-4.43	-.369	-.0505	4.3P
8	3.0P	3.9P	- .9	-4.98	-.415	-.0567	3.9P
9	2.1P	1.4P	+ .7	+3.88	+.323	+.0442	1.4P
10	2.6P	1.8P	+ .8	+4.43	+.369	+.0505	1.8P
11	1.5P	1.0P	+ .5	+2.75	+.229	+.0313	1.0P
12	6.0S	6.6S	+ .6	+3.32	+.277	+.0379	6.6S
13	5.4S	6.1S	+ .7	+3.88	+.323	+.0442	6.1S
14	4.9S	5.8S	+ .9	+4.98	+.415	+.0567	5.8S
15	3.9S	4.8S	+ .9	+4.98	+.415	+.0567	4.8S
16	2.0S	1.5S	- .5	-2.75	-.229	-.0313	1.5S
17*	1.0P	.6P	+ .4	+ .844	+.0703	+.0096	.6P
18	.5P	.3P	+ .2	+ .422	+.0352	+.0048	.3P
19	.5S	.2S	- .1	- .211	-.0176	-.00241	.3S
20	1.0S	.7S	- .3	- .633	-.0527	-.00721	.7S
21	1.5S	1.0S	- .5	-1.105	-.0921	-.0126	1.0S
22	2.0S	4.6S	+2.6	+5.75	+.479	+.0565	4.6S
23	1.7S	1.1S	- .6	-1.326	-.1105	-.0151	1.1S

* Spring change beginning with Run 17.

TABLE XIV

FIXED TRIM; FRONT PIVOTS

$\tau = 10.5^{\circ}$
$C_V = 2.34$
$C_\Delta = 0.8$
No Spray Strips

$\Delta = 4.36$
$+^{\circ} = .30$
$\Delta = 4.66$(lb.)

Run No.	ψ(Still), deg.	ψ(Moving), deg.	$\Delta\psi$	N, in.-lb.	N, ft.-lb.	N'	ψ, deg.
1	2.0S	2.9S	+.9	+4.98	+.415	+.0567	2.9S
2	1.5S	.9S	-.6	-3.32	-.277	-.0379	.9S
3	1.0S	.5S	-.5	-2.77	-.231	-.0316	.5S
4	.5S	.2S	-.3	-1.66	-.138	-.0189	.2S
5	.5P	.5P	0	0	0	0	.5P
6	1.1P	.9P	+.2	+1.11	+.0924	+.0126	.9P
7	1.5P	1.2P	+.3	+1.66	+.138	+.0189	1.2P
8	2.1P	1.5P	+.6	+3.32	+.277	+.0379	1.5P
9	1.6P	1.2P	+.4	+2.21	+.184	+.0252	1.2P

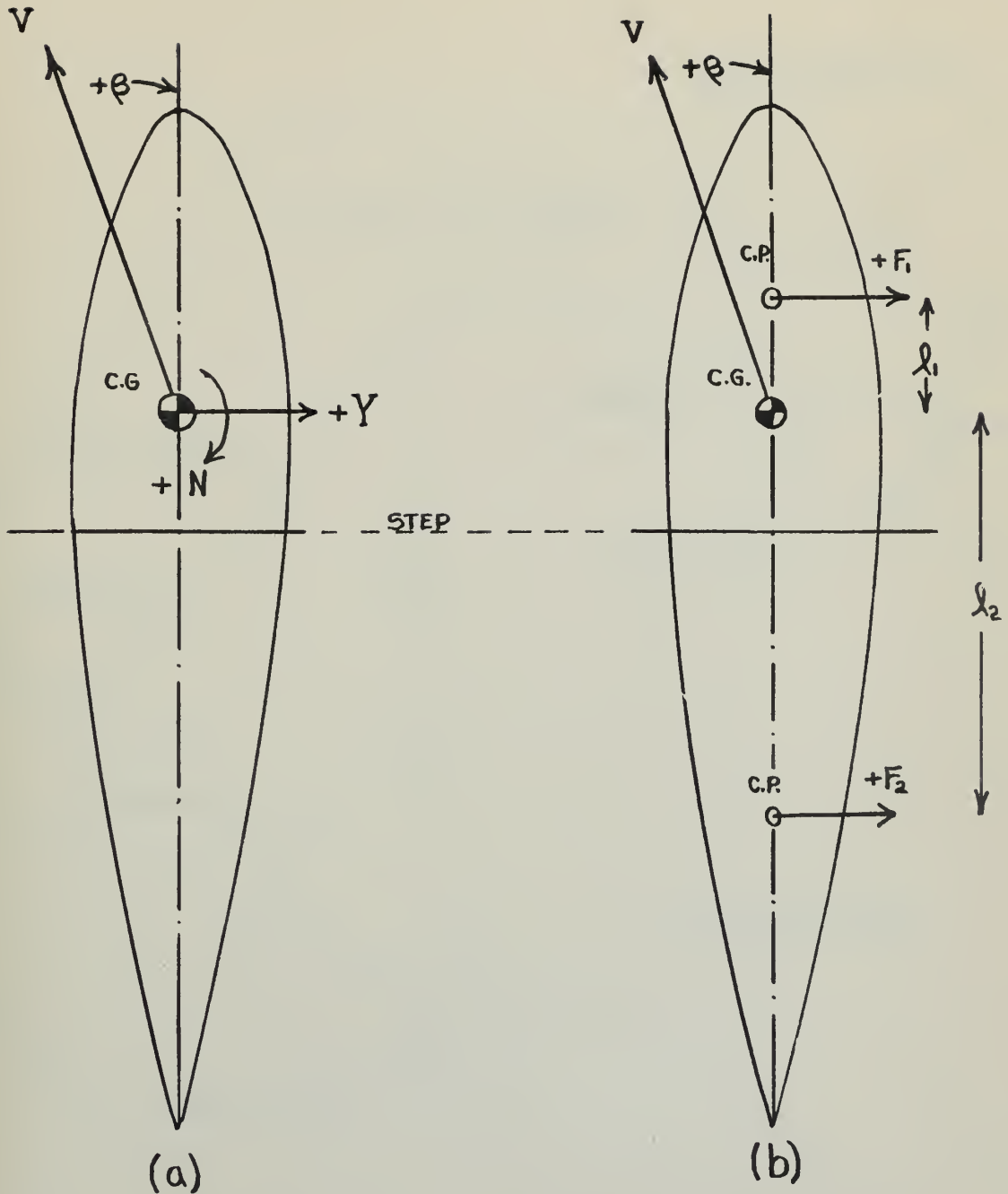

STATIC FORCES ON A
SEAPLANE HULL
AT A GIVEN ANGLE OF YAW

FIG. 1

DIAGRAMMATIC SKETCH OF SEAPLANE YAW APPARATUS

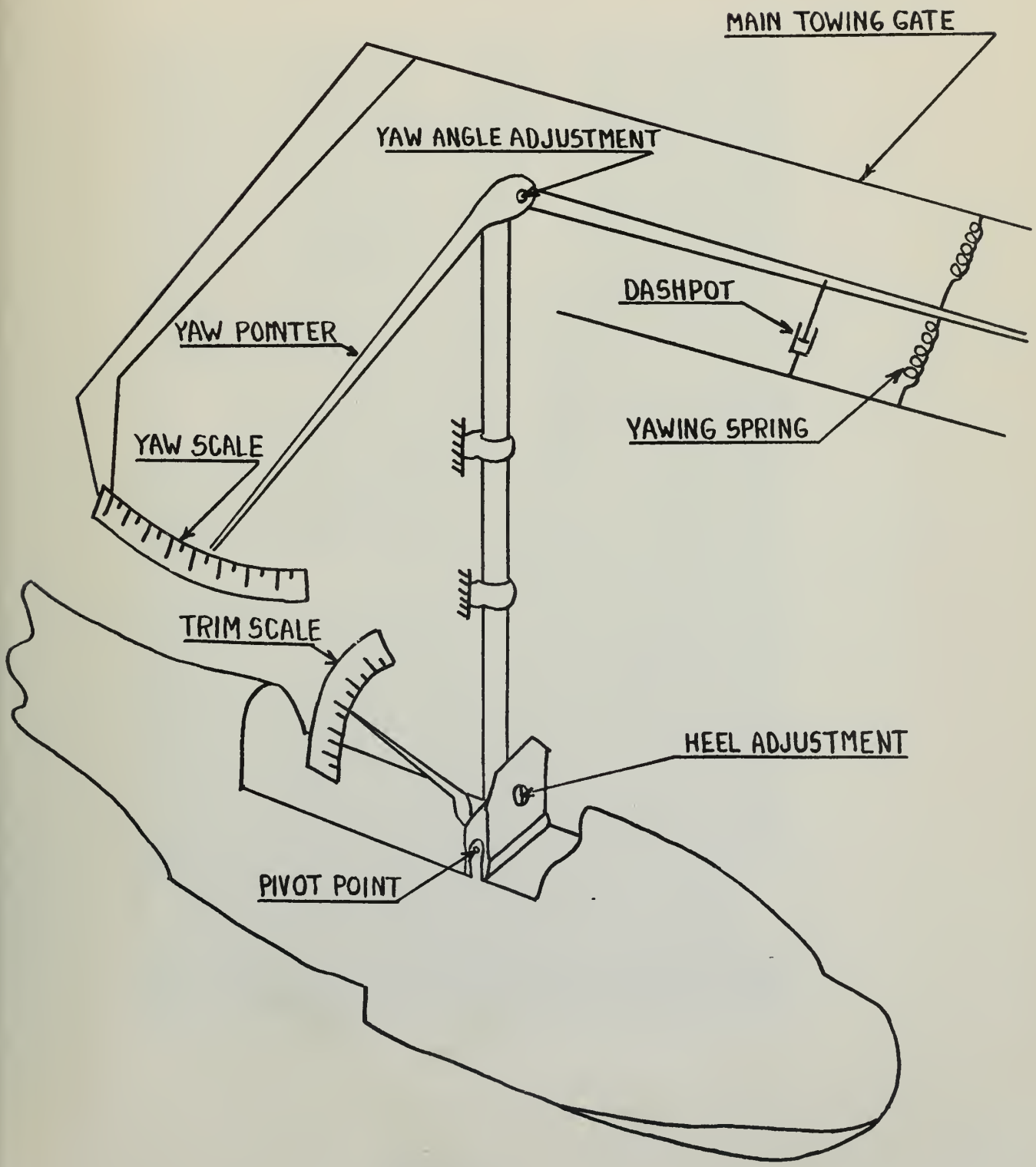

FIG. 2

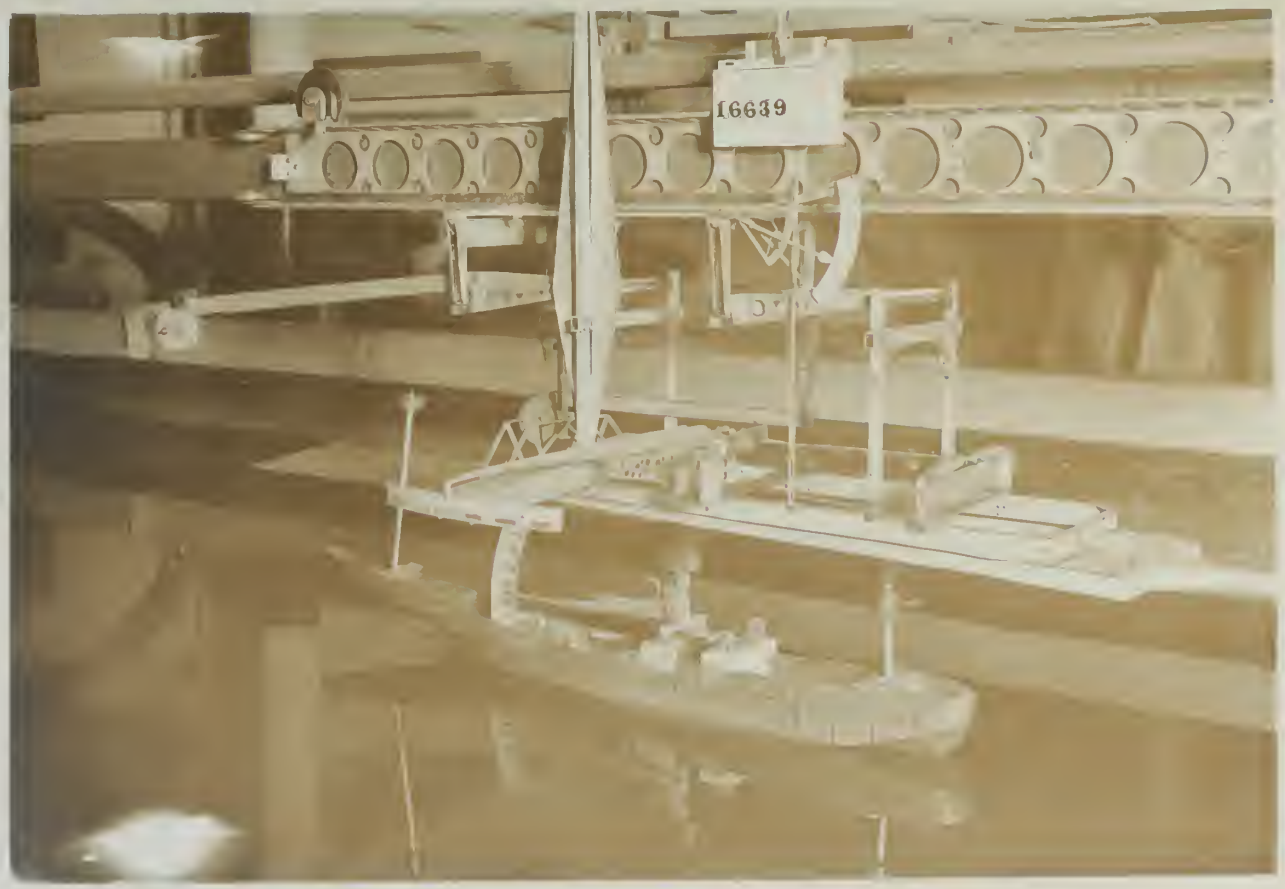

COMPLETE APPARATUS ARRANGEMENT

FIG. 3

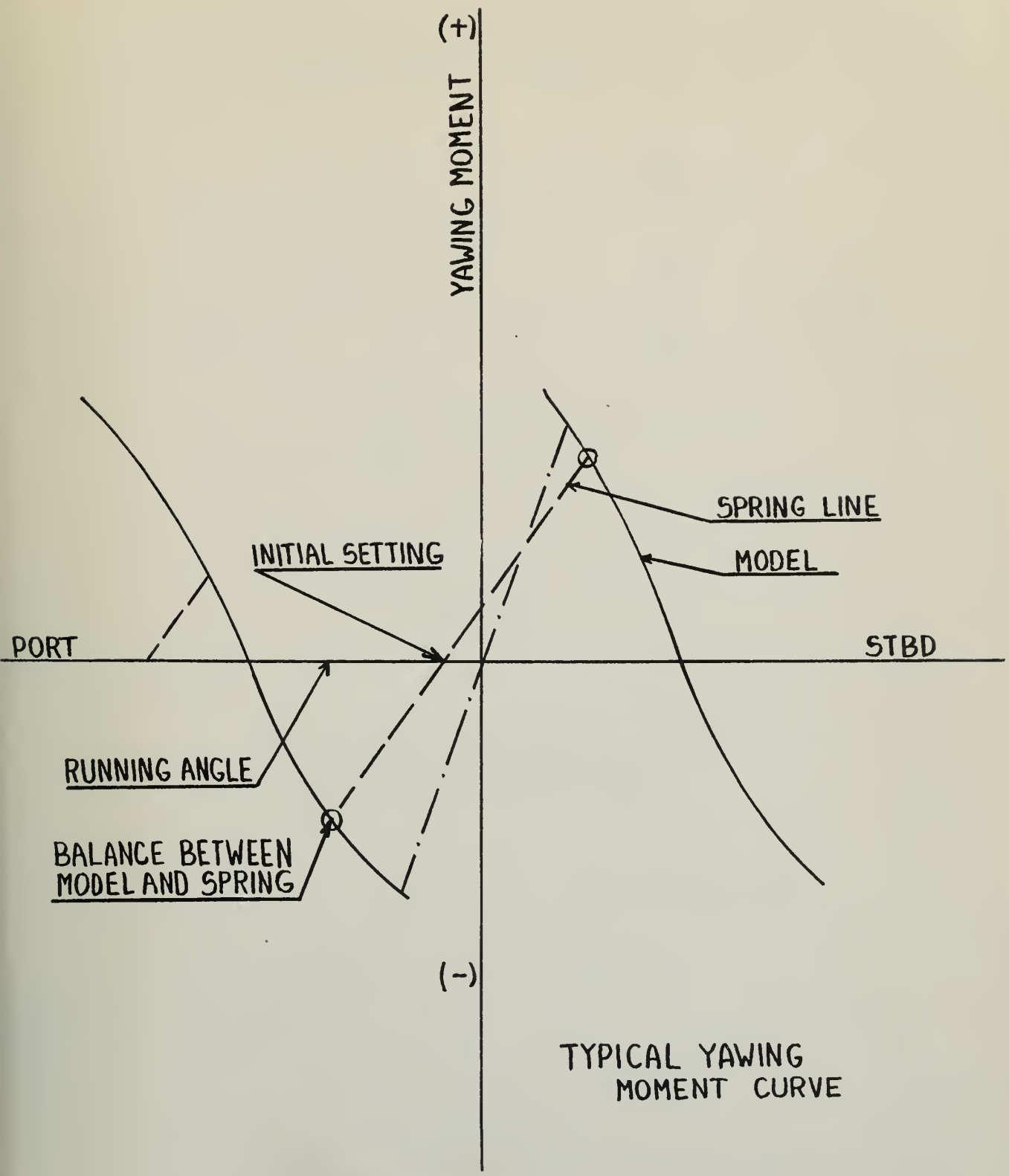
(+)
YAWING MOMENT
SPRING LINE
MODEL
INITIAL SETTING
PORT
STBD
RUNNING ANGLE
BALANCE BETWEEN
MODEL AND SPRING
(-)
TYPICAL YAWING
MOMENT CURVE

FIG. 4

SPRAY ROOT LINES

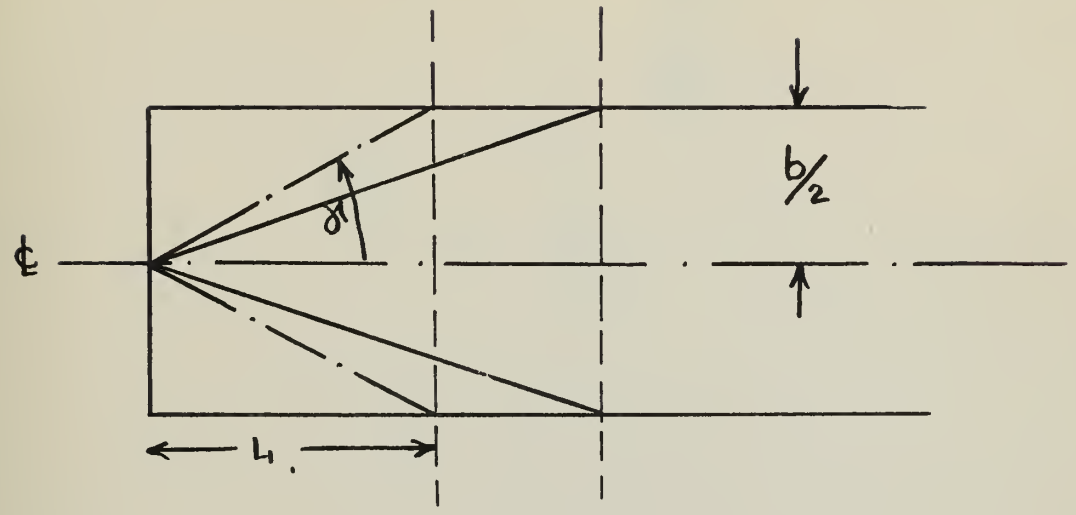

FIG. 5

REFERENCE DISTANCES FOR AFTERBODY BOTTOM

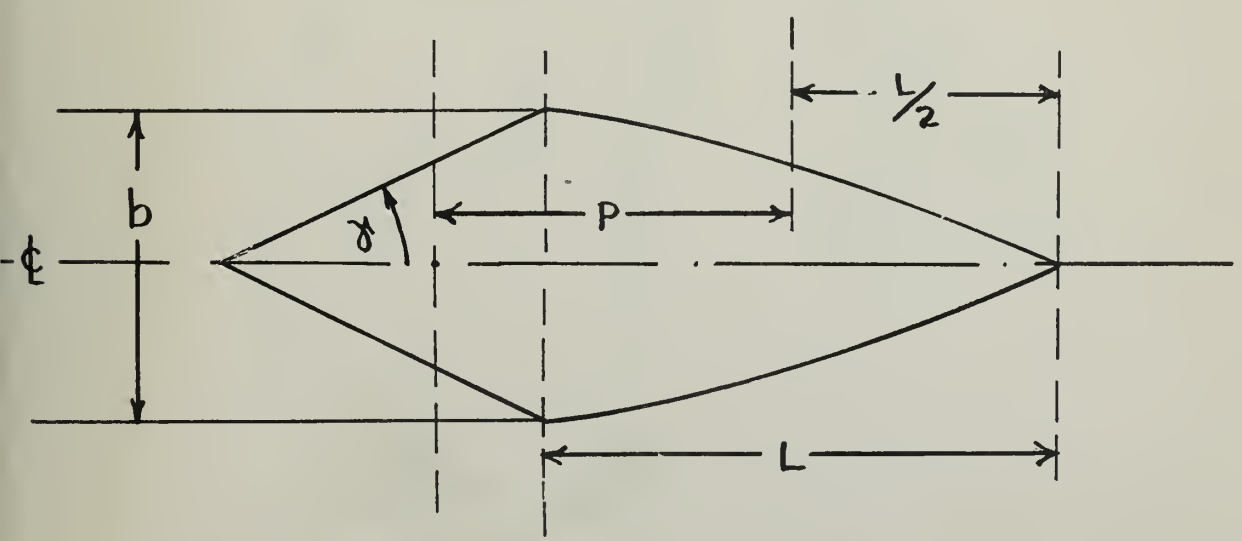

FIG. 6

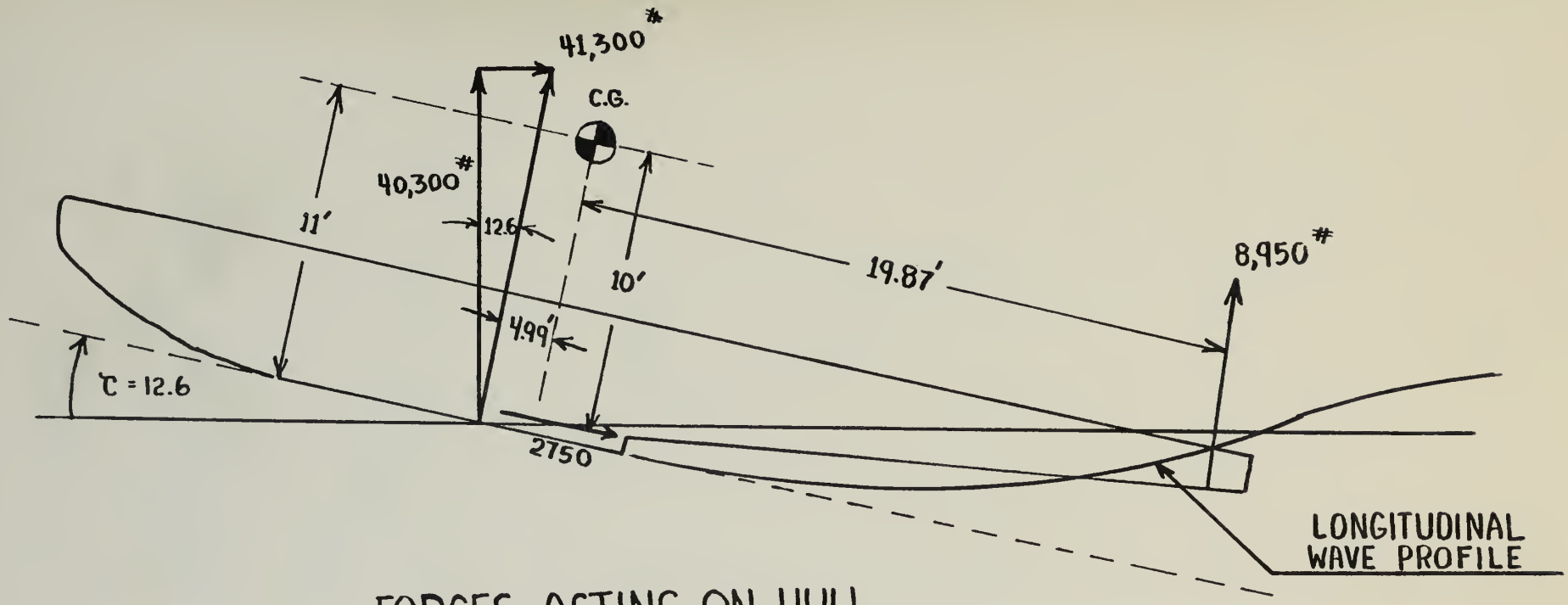

FORCES ACTING ON HULL
IN PLANING CONDITION

$C_V = 2.63$
$C_\Delta = 0.8$

FIG. 7

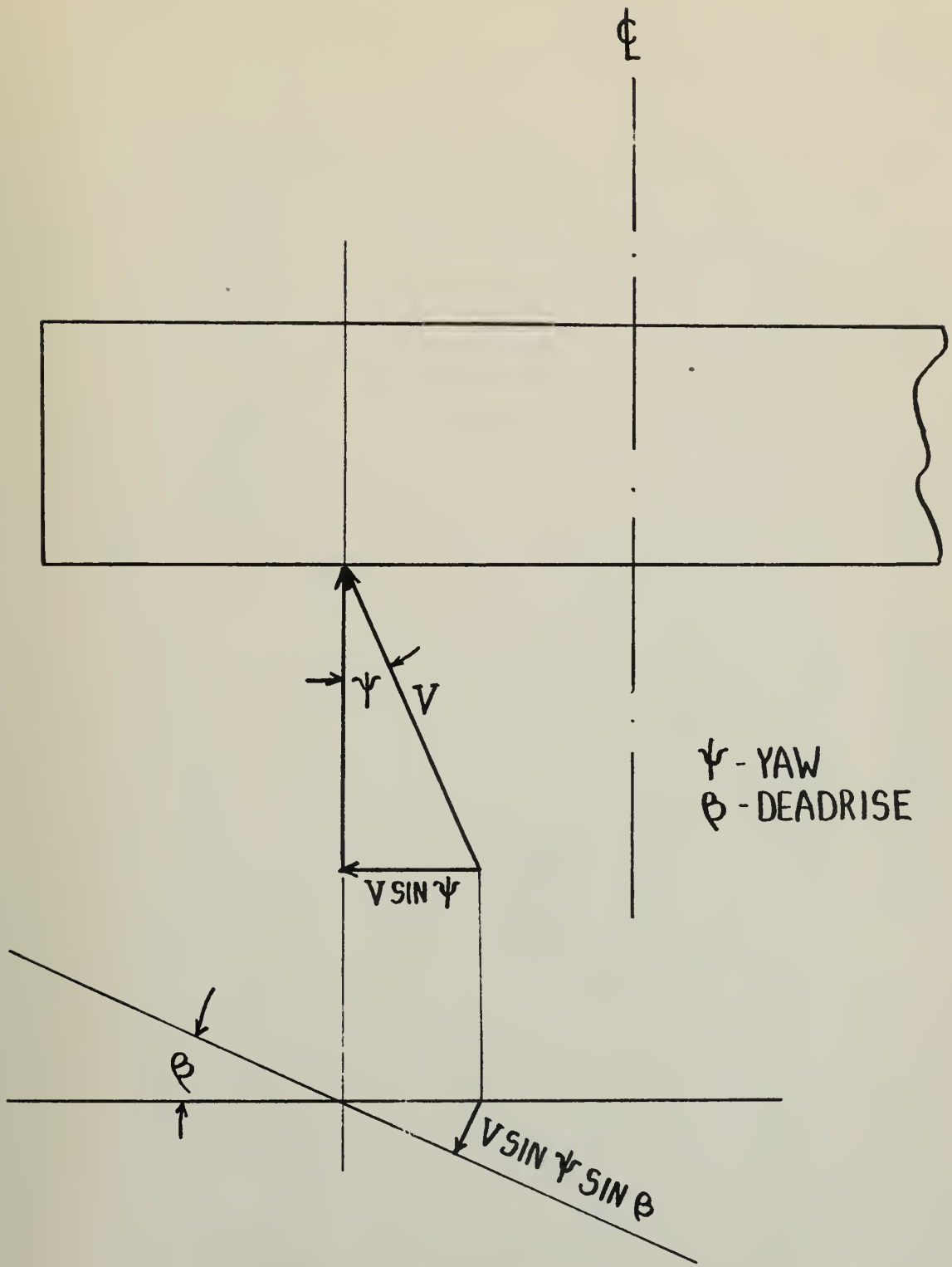

CHANGE IN TRIM ANGLE
DUE TO YAW

FIG. 8

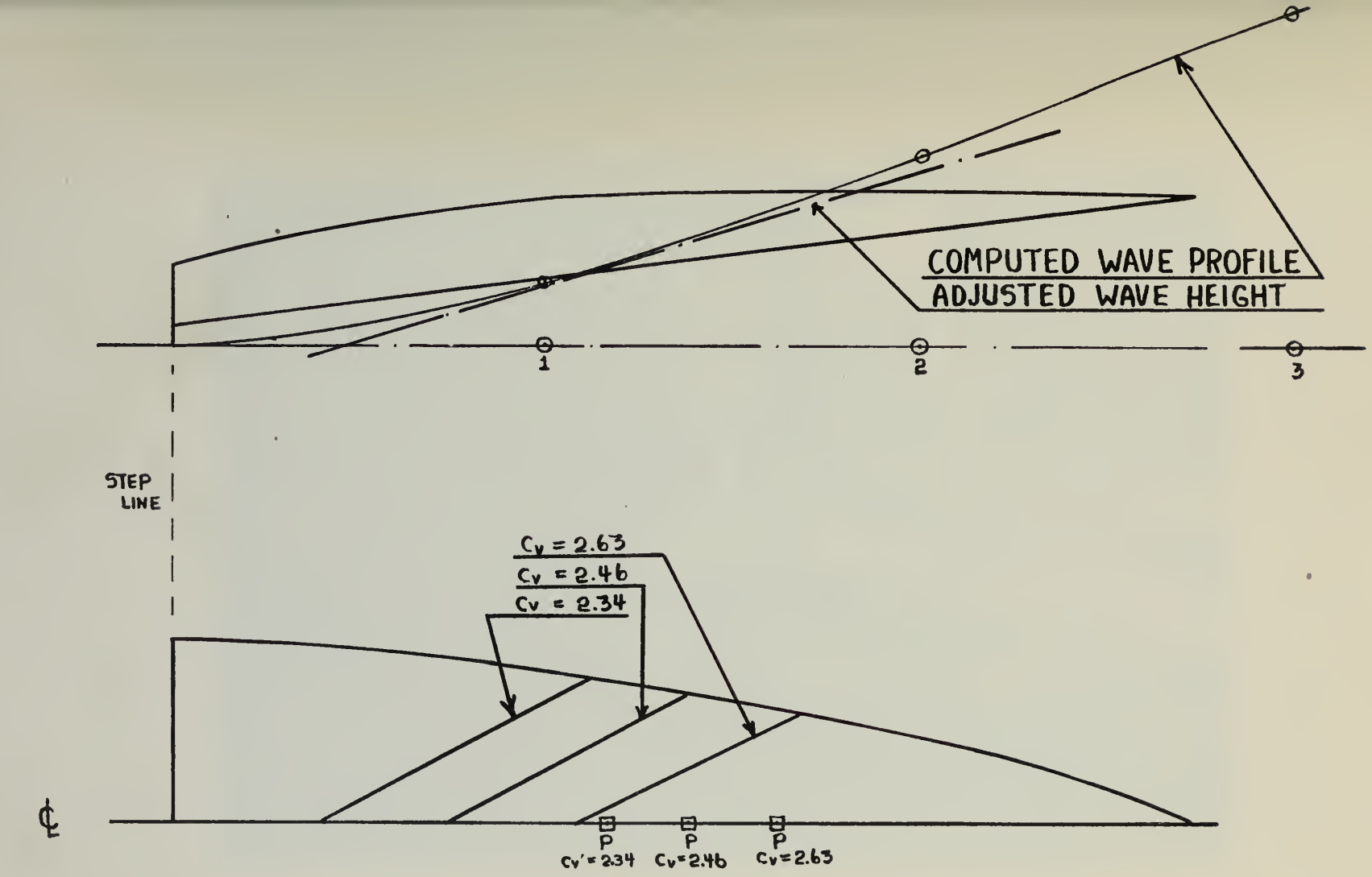

AFTERBODY PLAN

WETTED AREAS

FIG. 9

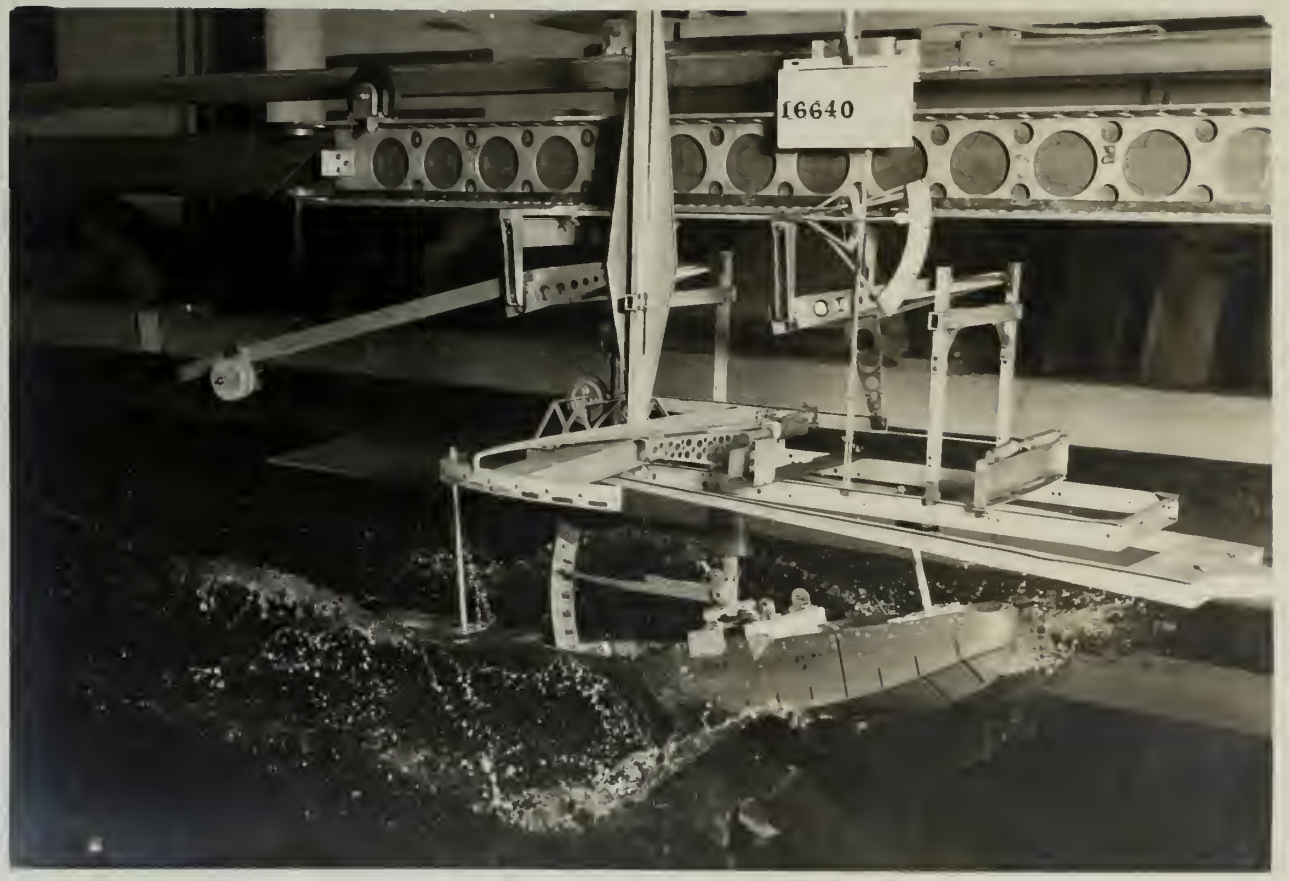

FIG. 10

$C_\Delta = 0.8$

$C_V = 2.63$

$\Psi = 6.35$

HULL FORCE DIAGRAMS

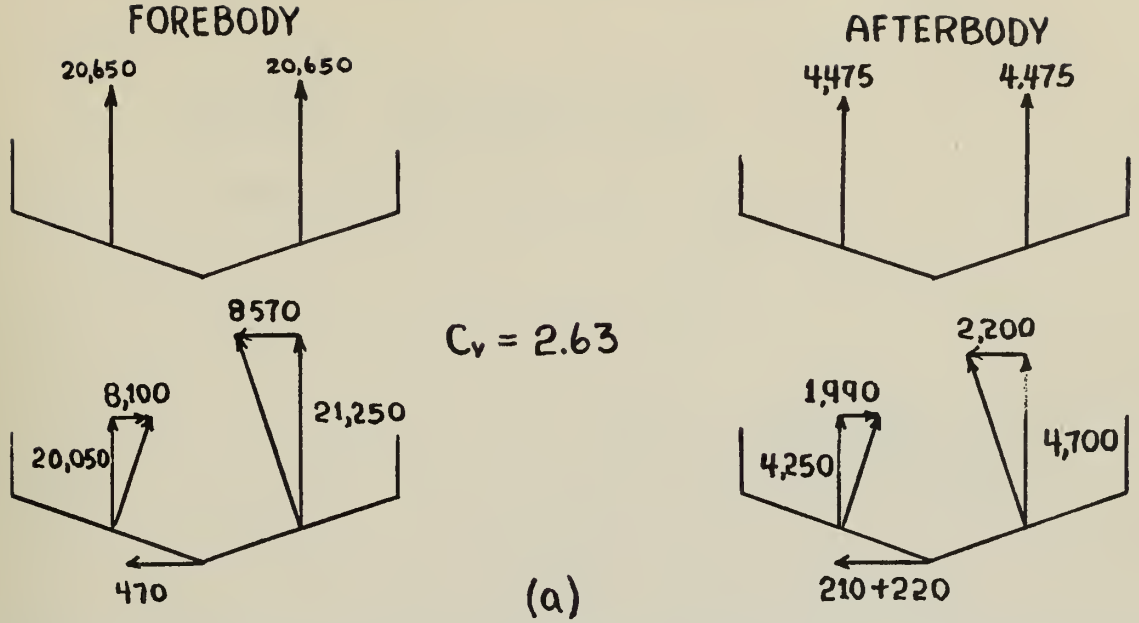

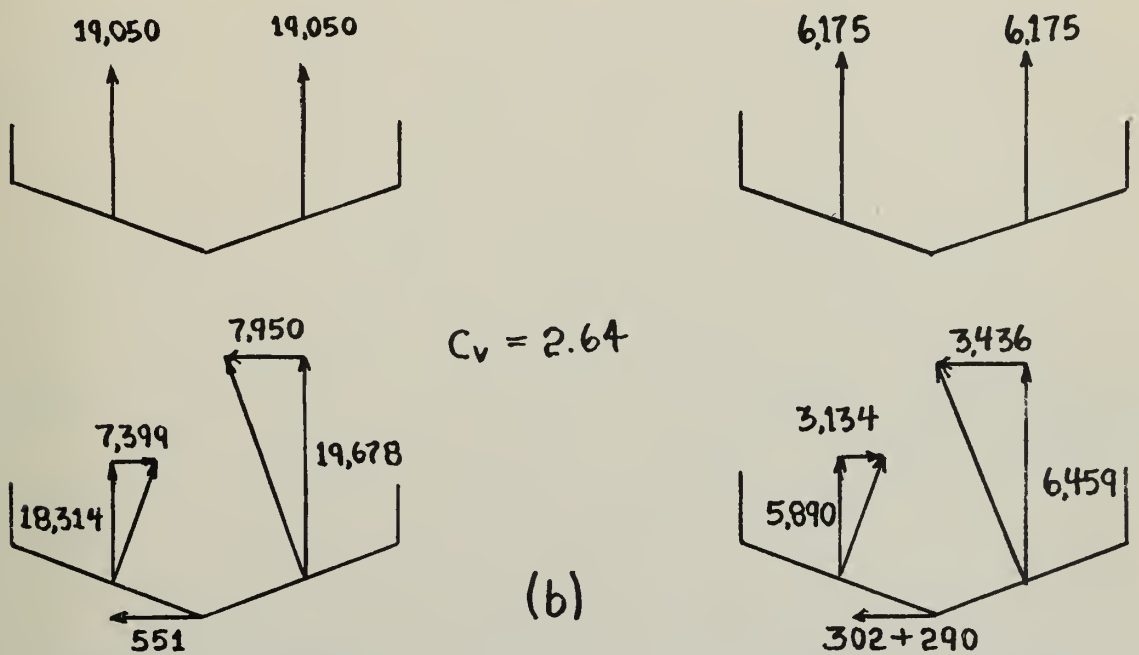

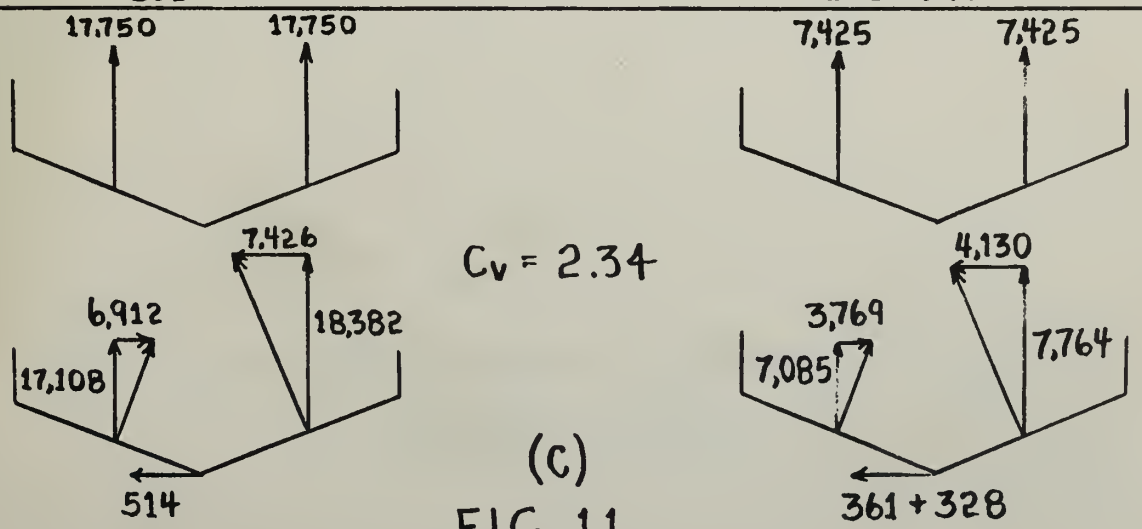

FIG. 11

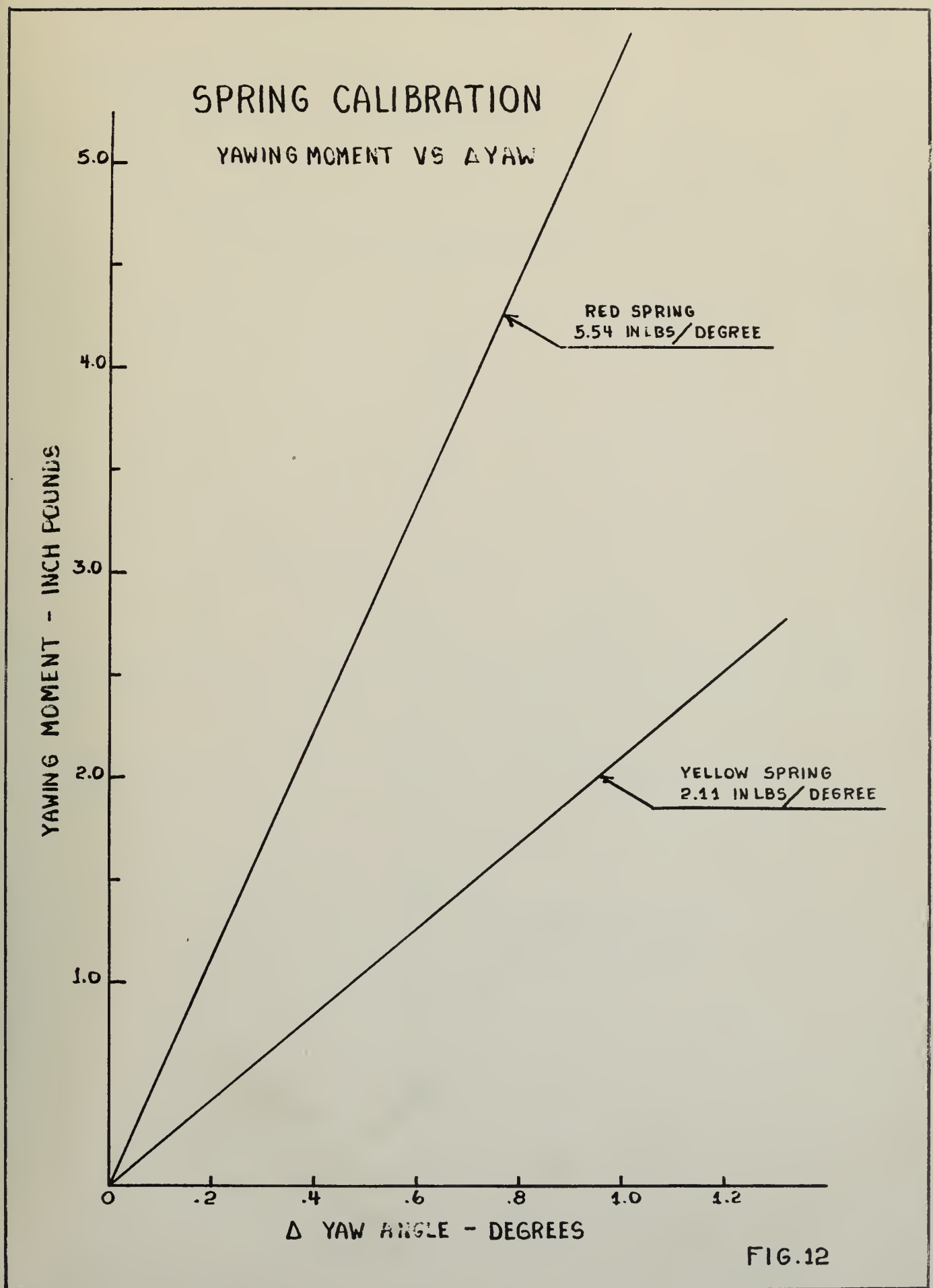
SPRING CALIBRATION
YAWING MOMENT VS ΔYAW
5.0
4.0
3.0
2.0
1.0
YAWING MOMENT - INCH POUNDS
RED SPRING
5.54 IN LBS/DEGREE
YELLOW SPRING
2.11 IN LBS/DEGREE
0
.2
.4
.6
.8
1.0
1.2
Δ YAW ANGLE - DEGREES

FIG. 12

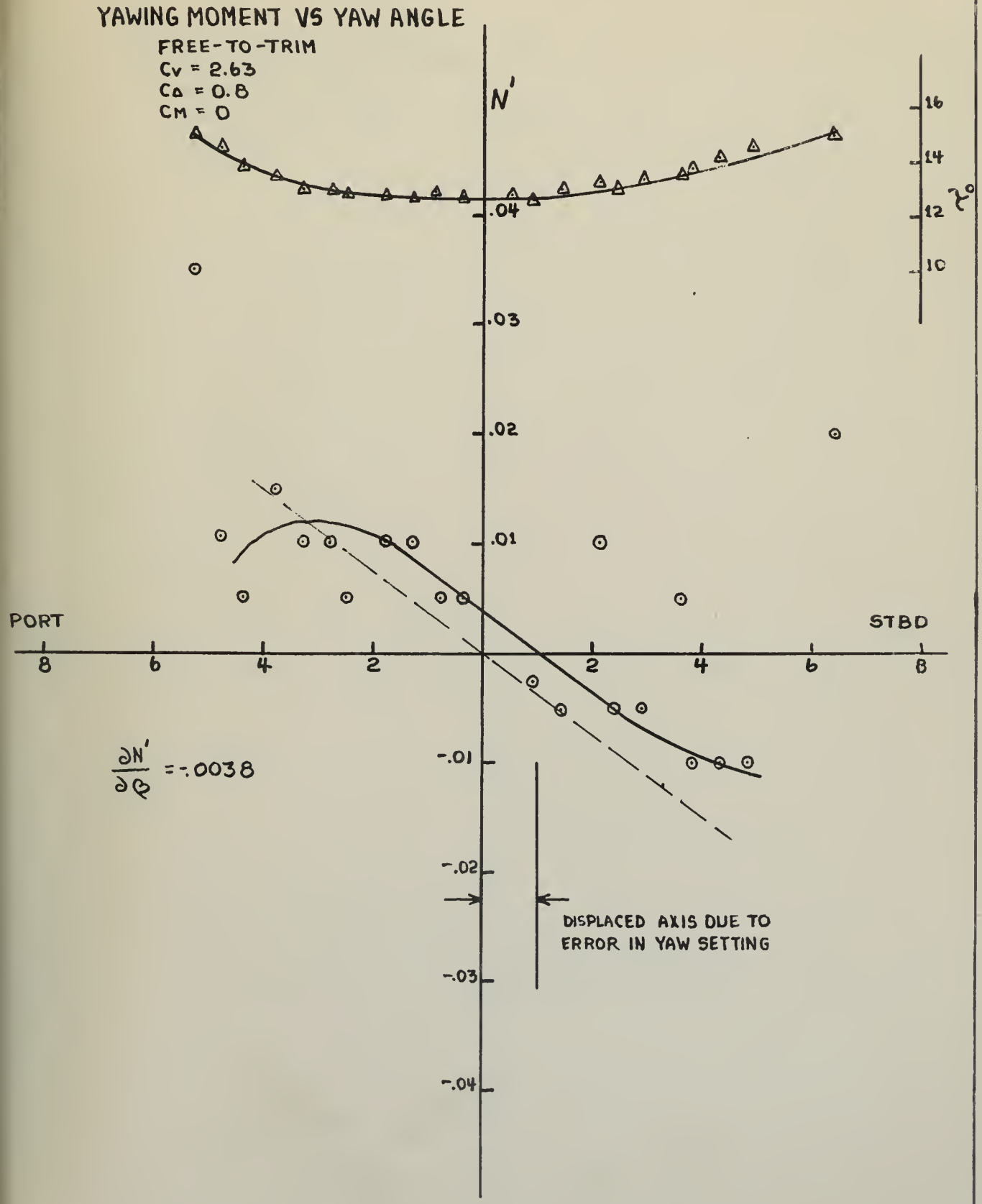
YAWING MOMENT VS YAW ANGLE
FREE-TO-TRIM
Cv = 2.63
Cδ = 0.8
CM = 0
N'
.04
.03
.02
.01
-.01
-.02
-.03
-.04
16
14
12
10
γ°
PORT
STBD
8
6
4
2
2
4
6
8
∂N'/∂β = -.0038
DISPLACED AXIS DUE TO
ERROR IN YAW SETTING

FIG. 13

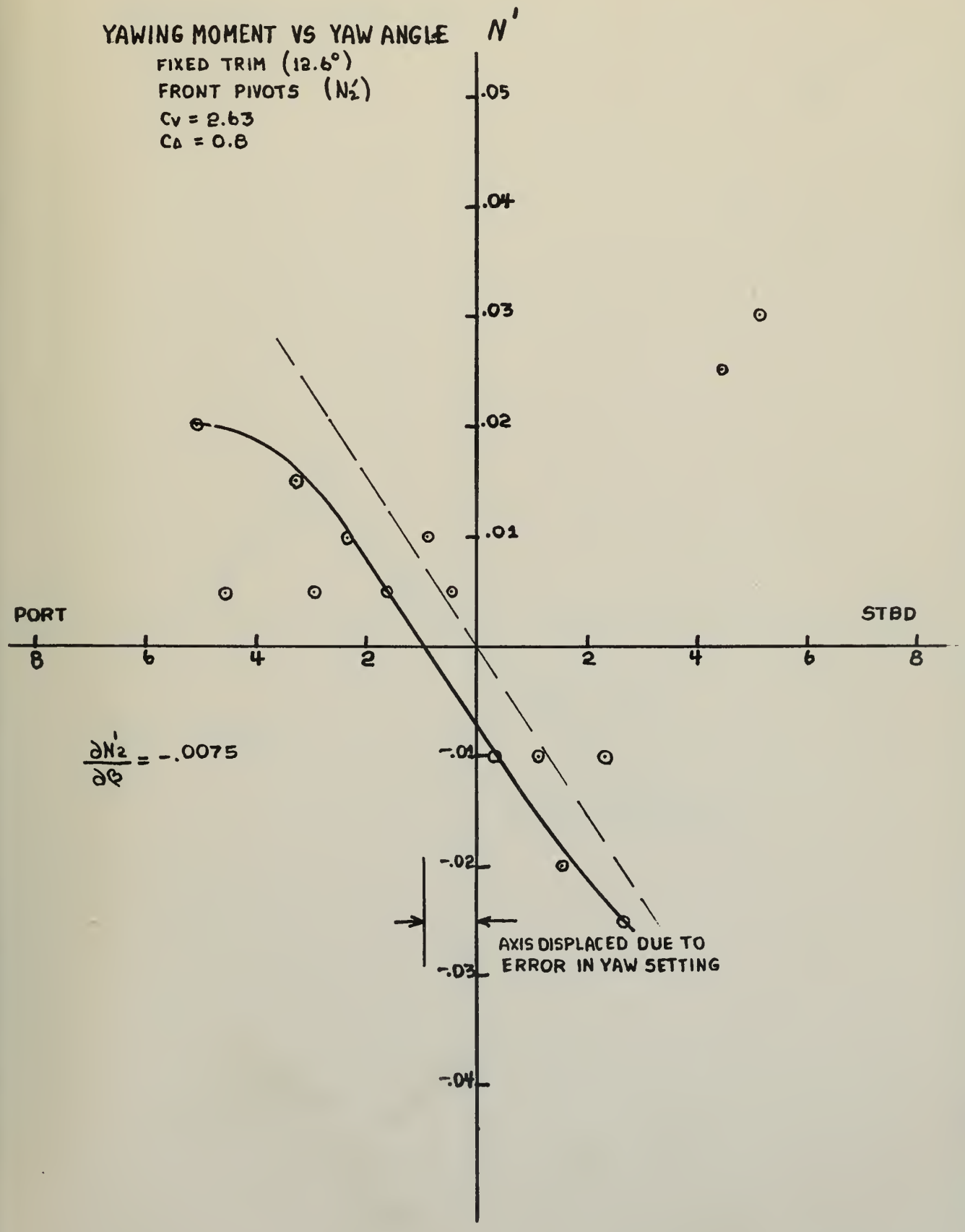
YAWING MOMENT VS YAW ANGLE N'
FIXED TRIM (12.6°)
FRONT PIVOTS (N'2)
Cv = 2.63
CΔ = 0.8
.05
.04
.03
.02
.01
-.01
-.02
-.03
-.04
PORT
STBD
8
6
4
2
2
4
6
8
∂N'2/∂Ψ = -.0075
AXIS DISPLACED DUE TO
ERROR IN YAW SETTING

FIG. 14

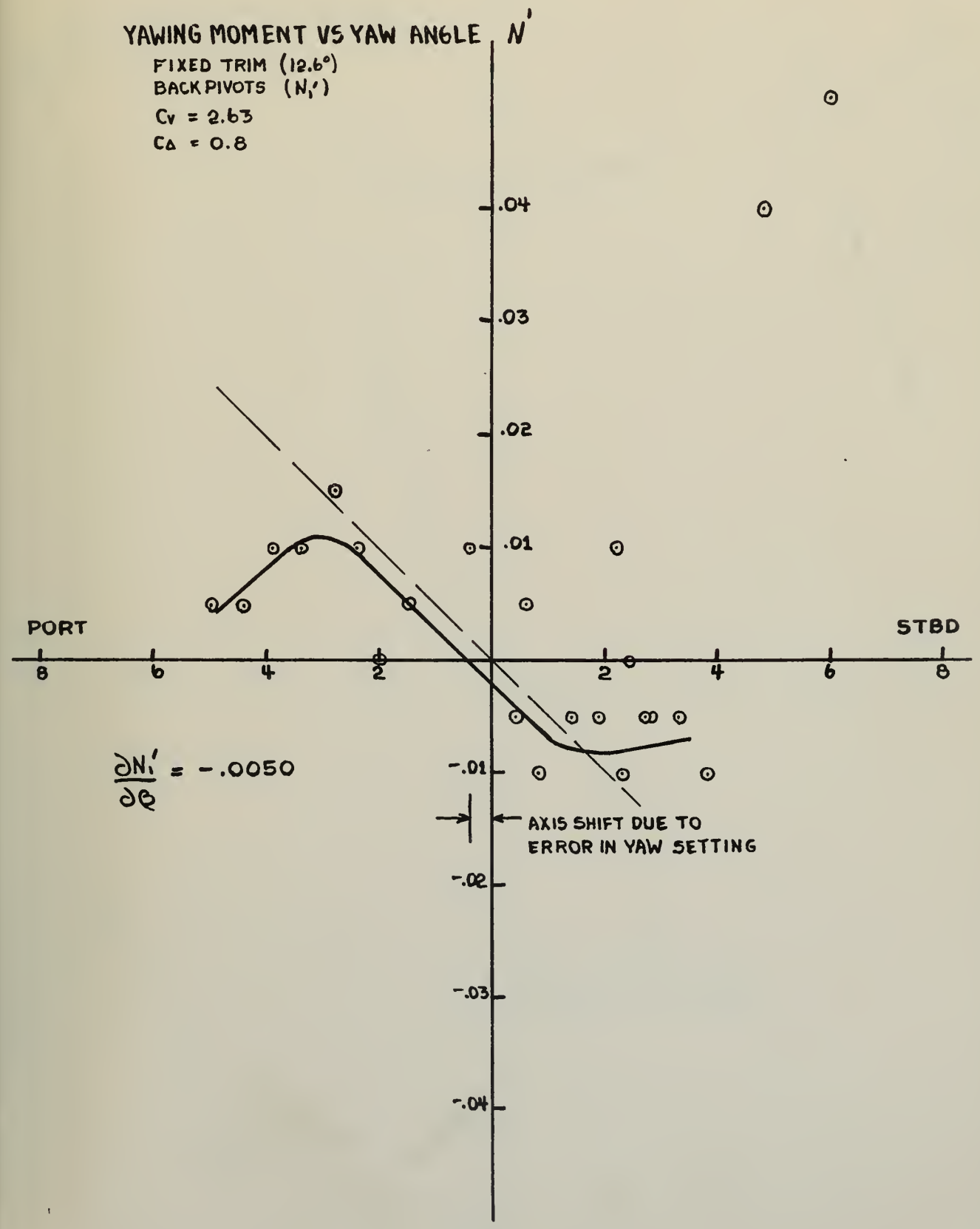
YAWING MOMENT VS YAW ANGLE N'
FIXED TRIM (12.6°)
BACK PIVOTS (N₁')
Cv = 2.63
CΔ = 0.8
.04
.03
.02
.01
-.01
-.02
-.03
-.04
PORT
STBD
8
6
4
2
2
4
6
8
∂N₁'/∂Θ = -.0050
AXIS SHIFT DUE TO
ERROR IN YAW SETTING

FIG. 15

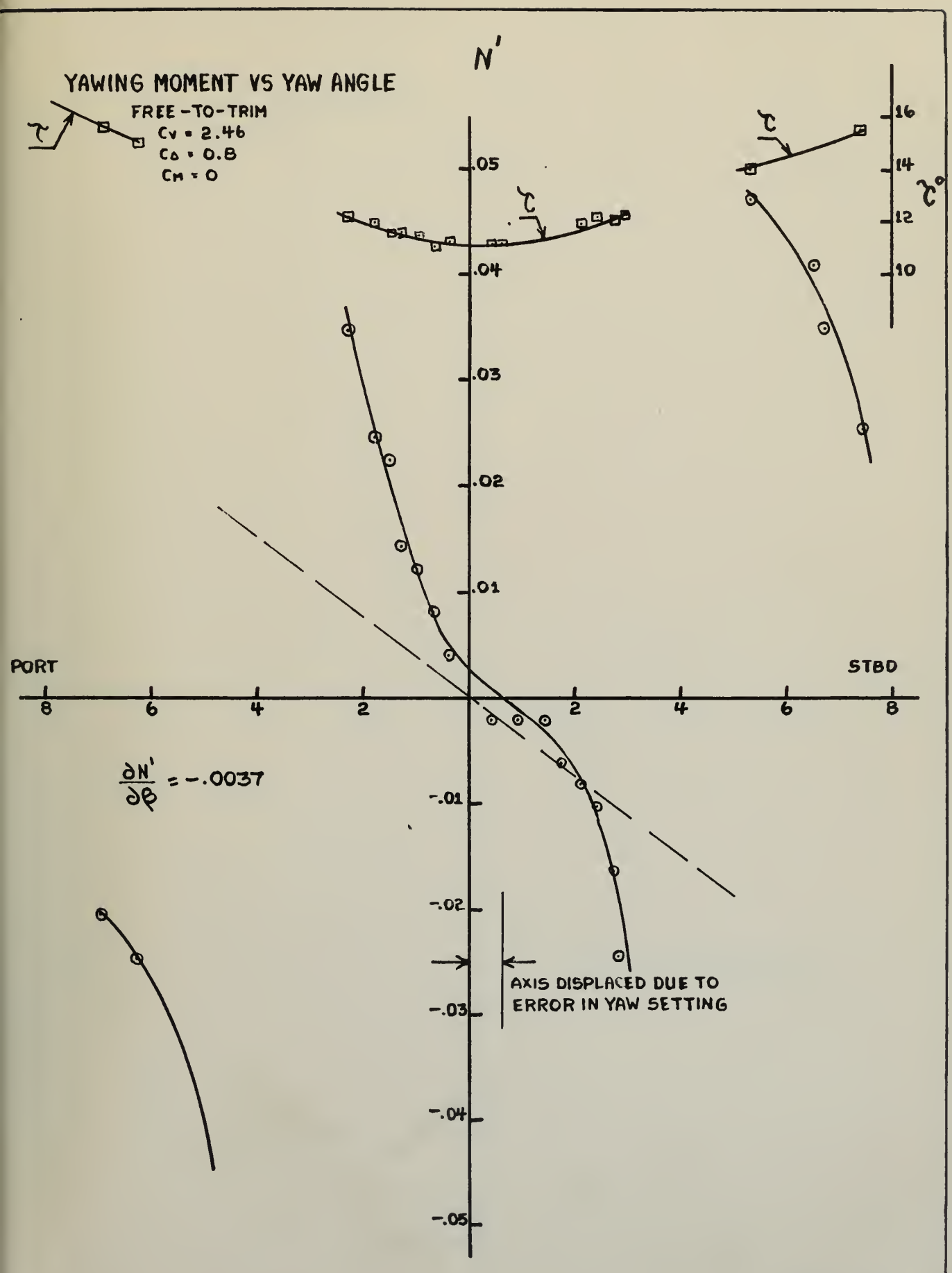
N'
YAWING MOMENT VS YAW ANGLE
FREE-TO-TRIM
Cv = 2.46
Cδ = 0.8
CM = 0
τ
.05
.04
.03
.02
.01
-.01
-.02
-.03
-.04
-.05
16
14
12
10
τ°
PORT
STBD
8
6
4
2
2
4
6
8
∂N'/∂β = -.0037
AXIS DISPLACED DUE TO
ERROR IN YAW SETTING

FIG. 16

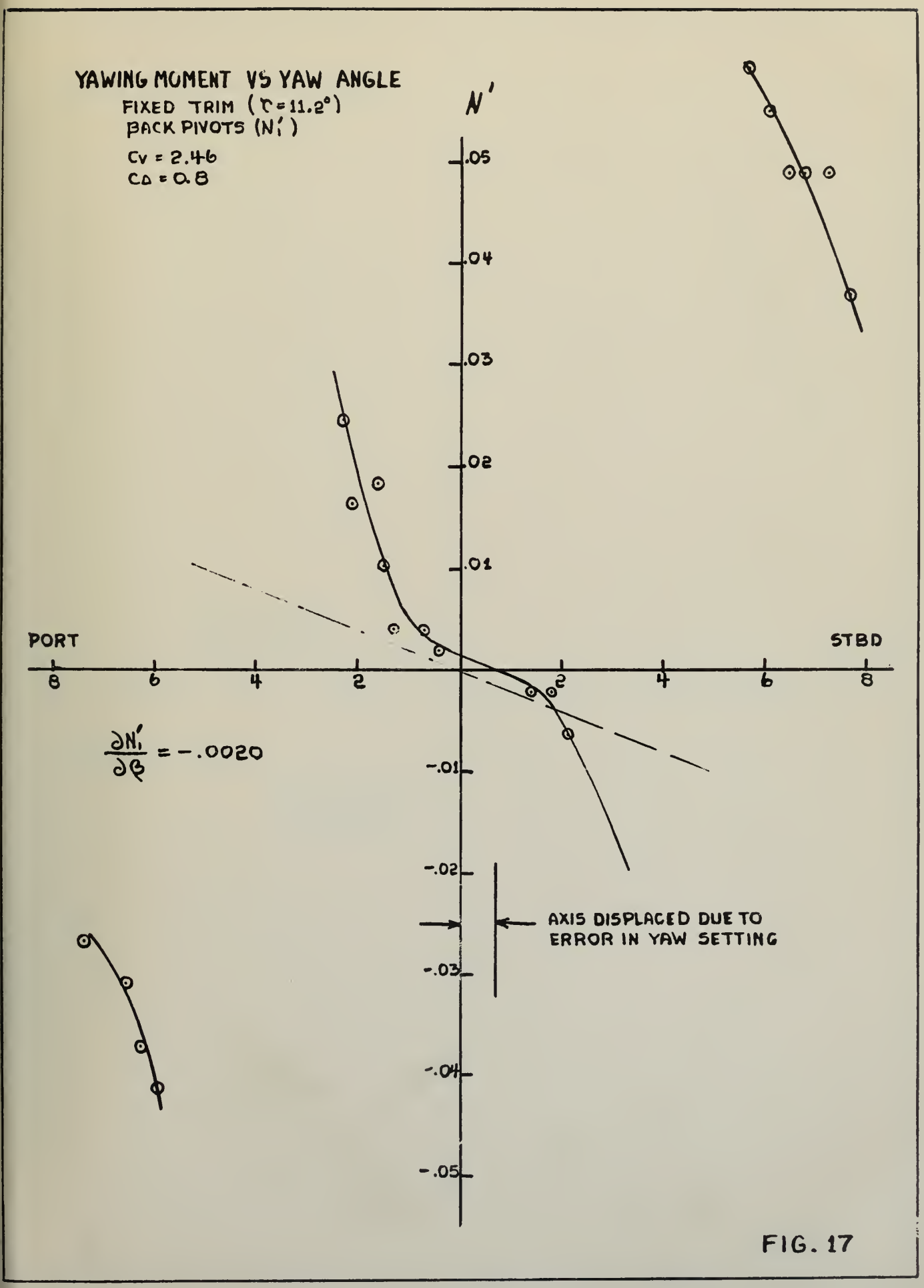
YAWING MOMENT VS YAW ANGLE
FIXED TRIM (τ = 11.2°)
BACK PIVOTS (N'1)
Cv = 2.46
CD = 0.8
N'
.05
.04
.03
.02
.01
PORT
STBD
8
6
4
2
2
4
6
8
∂N'1/∂β = −.0020
-.01
-.02
-.03
-.04
-.05
AXIS DISPLACED DUE TO
ERROR IN YAW SETTING

FIG. 17

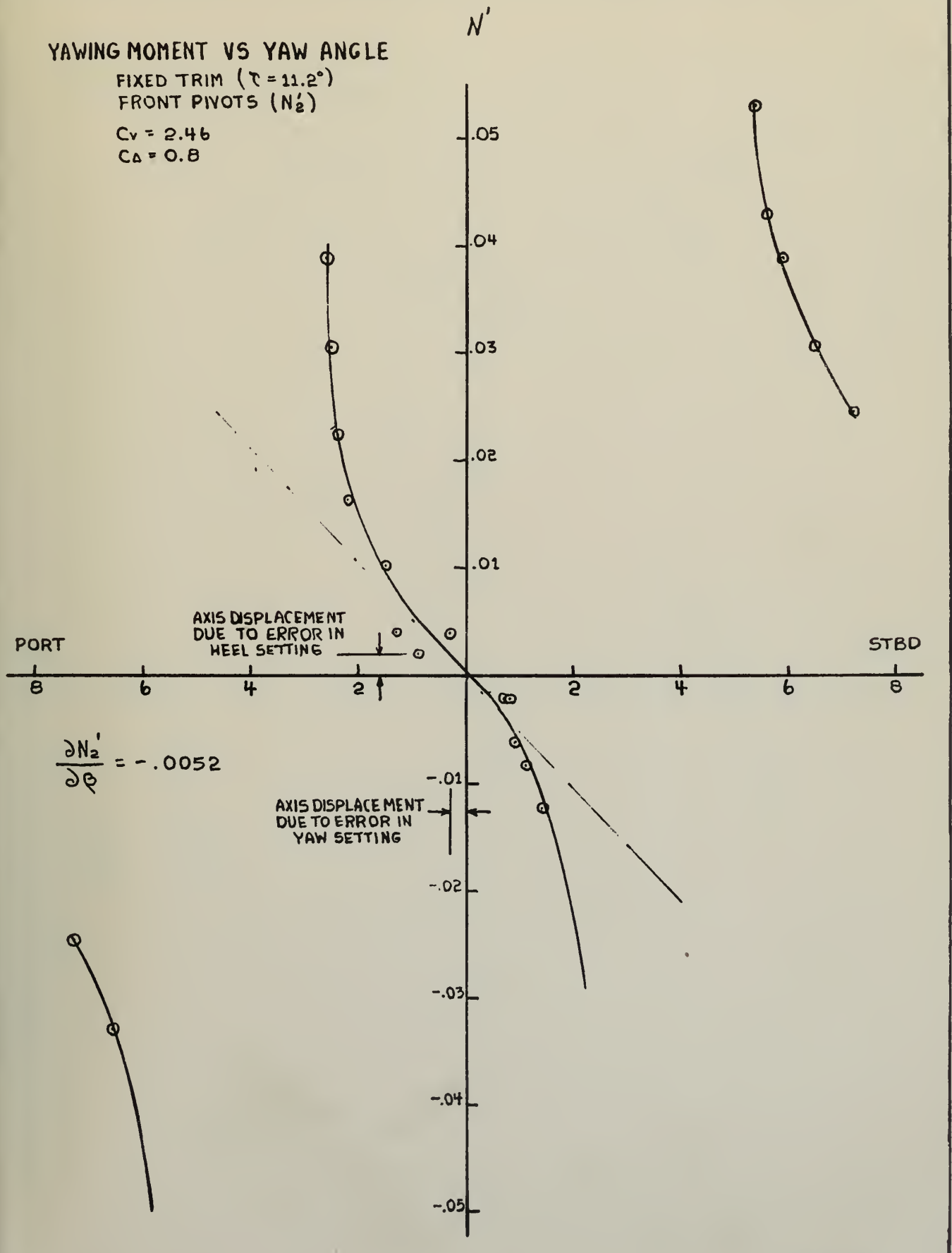
N'
YAWING MOMENT VS YAW ANGLE
FIXED TRIM (τ = 11.2°)
FRONT PIVOTS (N'2)
Cv = 2.46
CΔ = 0.8
.05
.04
.03
.02
.01
-.01
-.02
-.03
-.04
-.05
PORT
STBD
8
6
4
2
2
4
6
8
AXIS DISPLACEMENT DUE TO ERROR IN HEEL SETTING
AXIS DISPLACEMENT DUE TO ERROR IN YAW SETTING
∂N'2/∂θ = -.0052

FIG.18

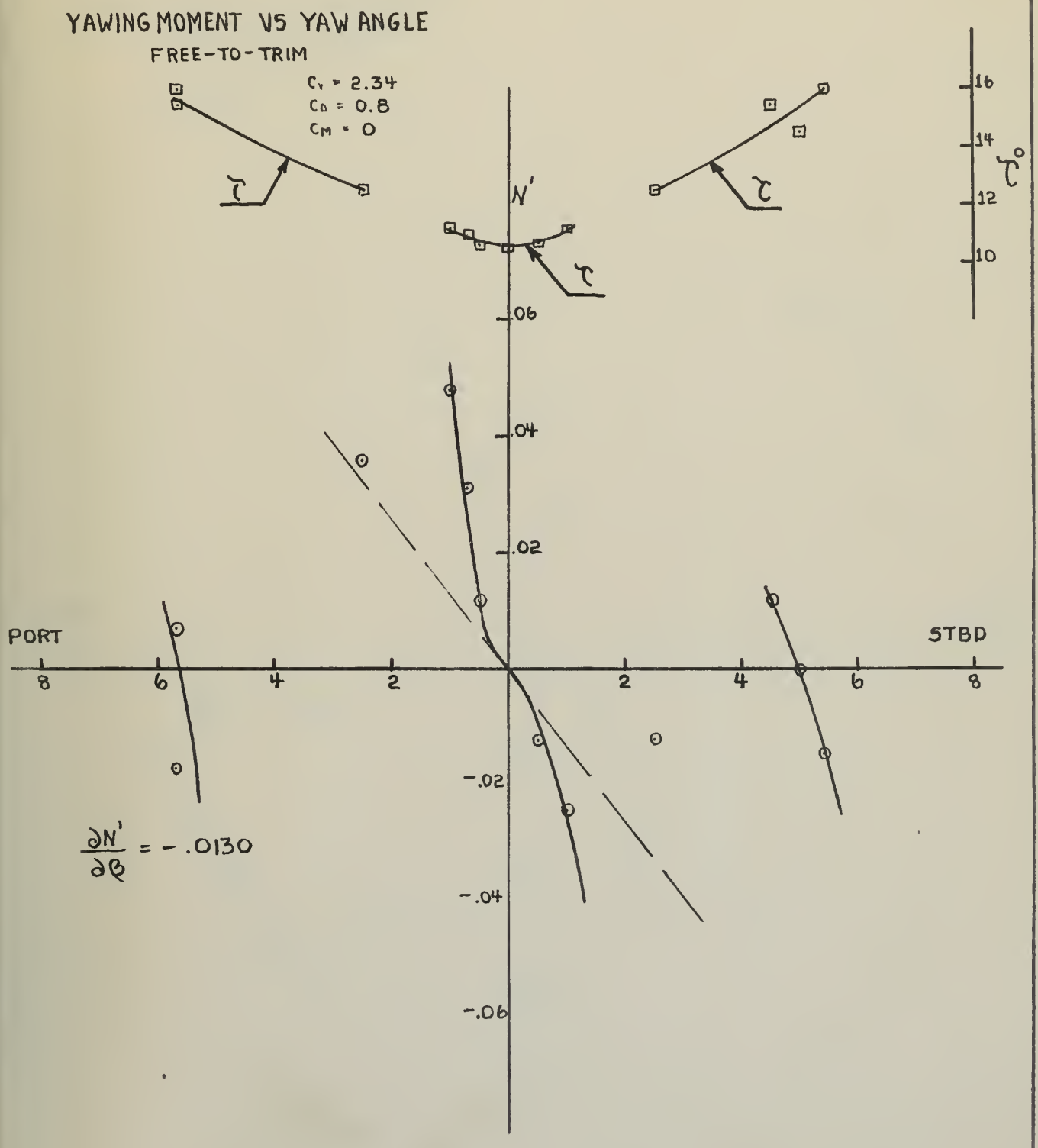
YAWING MOMENT VS YAW ANGLE
FREE-TO-TRIM
C_Y = 2.34
C_D = 0.8
C_M = 0
τ
N'
τ
τ
16
14
12
10
$\tau°$
.06
.04
.02
PORT
STBD
8
6
4
2
2
4
6
8
-.02
-.04
-.06
$\frac{\partial N'}{\partial \beta} = -.0130$

FIG. 19

YAWING MOMENT VS YAW ANGLE

FIXED TRIM ($\tau = 10.5°$)

BACK PIVOTS (N_1')

$C_V = 2.34$

$C_\Delta = 0.8$

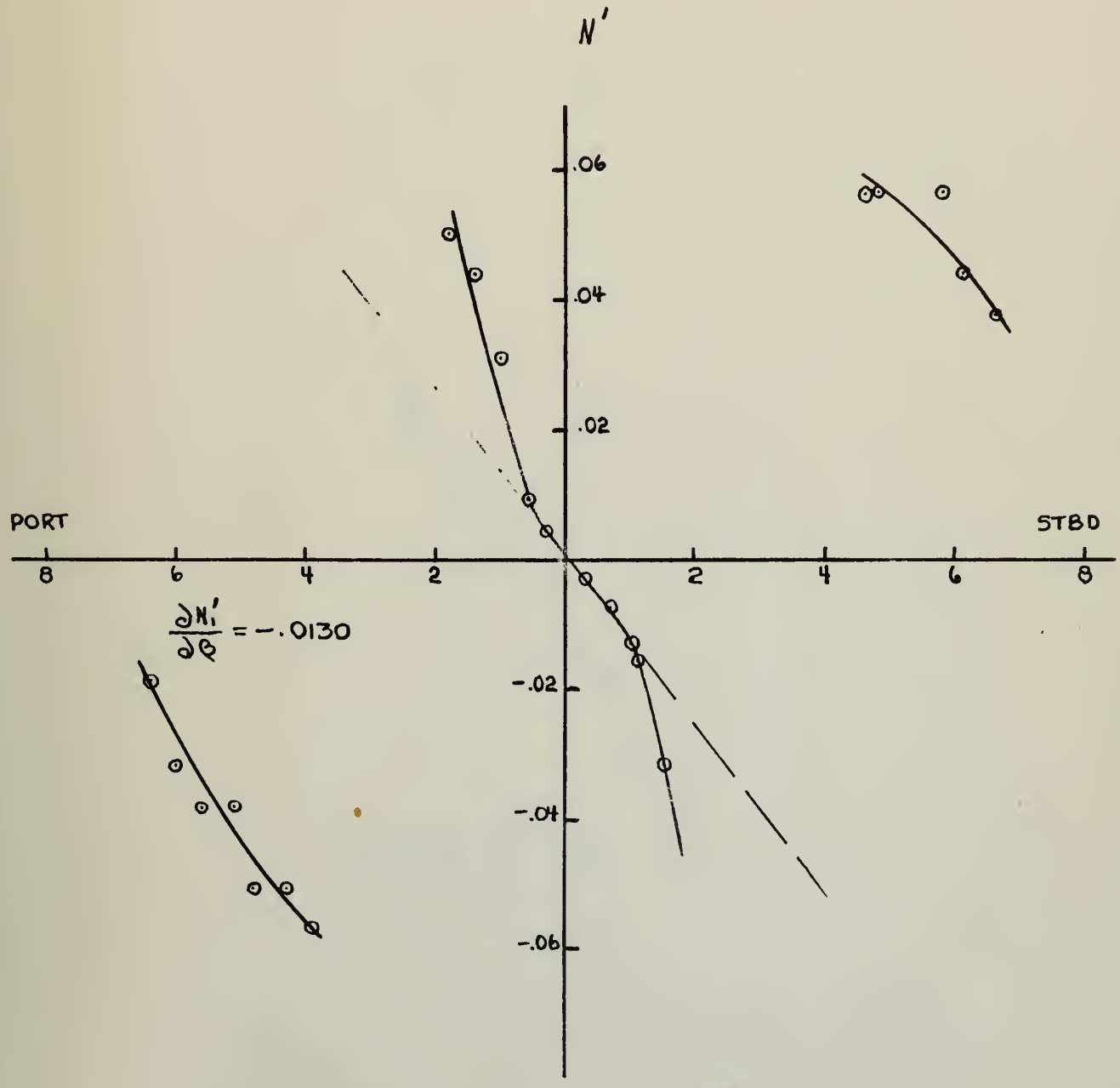

FIG. 20

YAWING MOMENT VS YAW ANGLE

FIXED TRIM ($\tau = 10.5°$)

FRONT PIVOTS (N_2')

$C_V = 2.34$

$C_\Delta = 0.8$

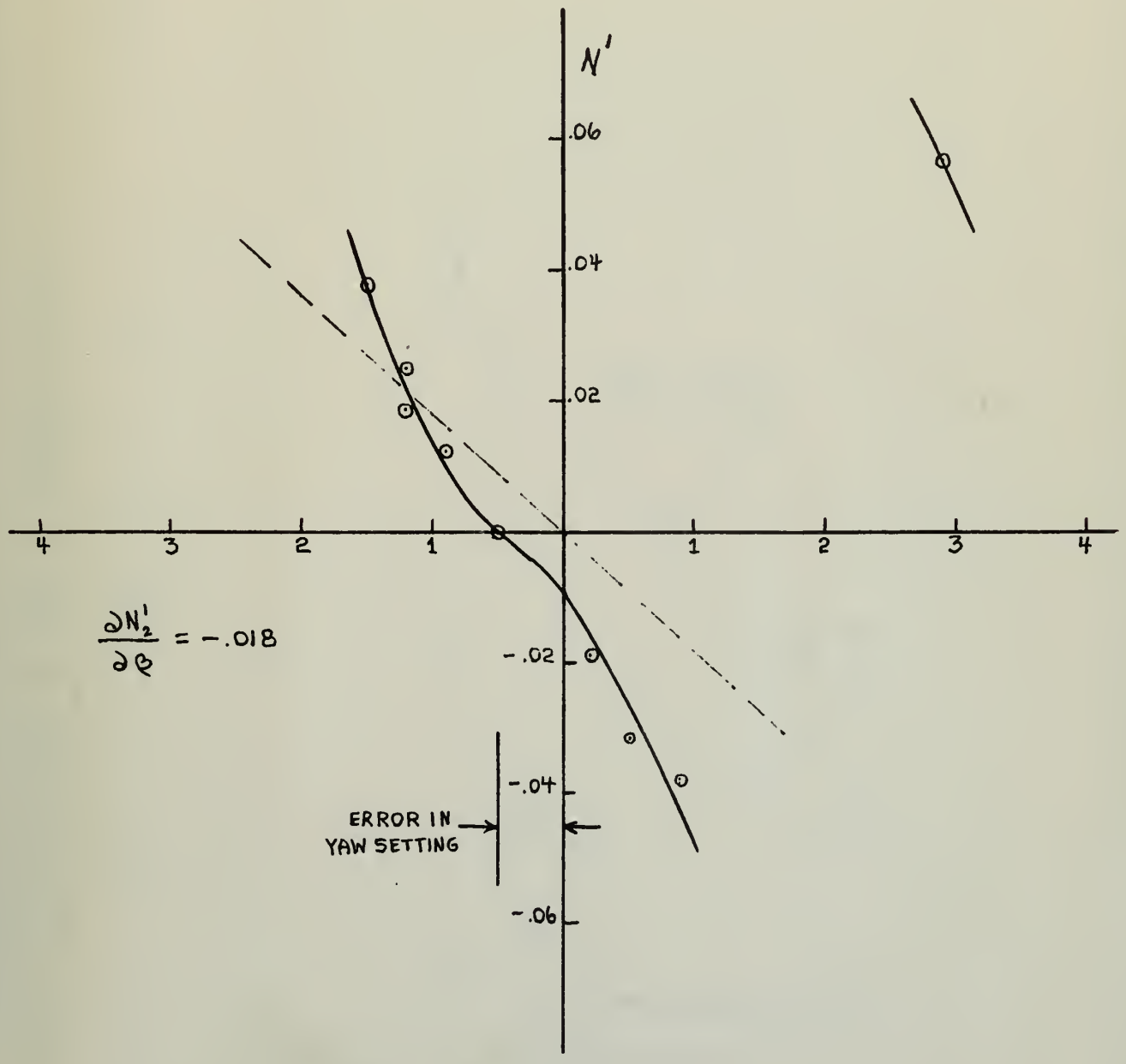

$\frac{\partial N_2'}{\partial \psi} = -.018$

FIG. 21

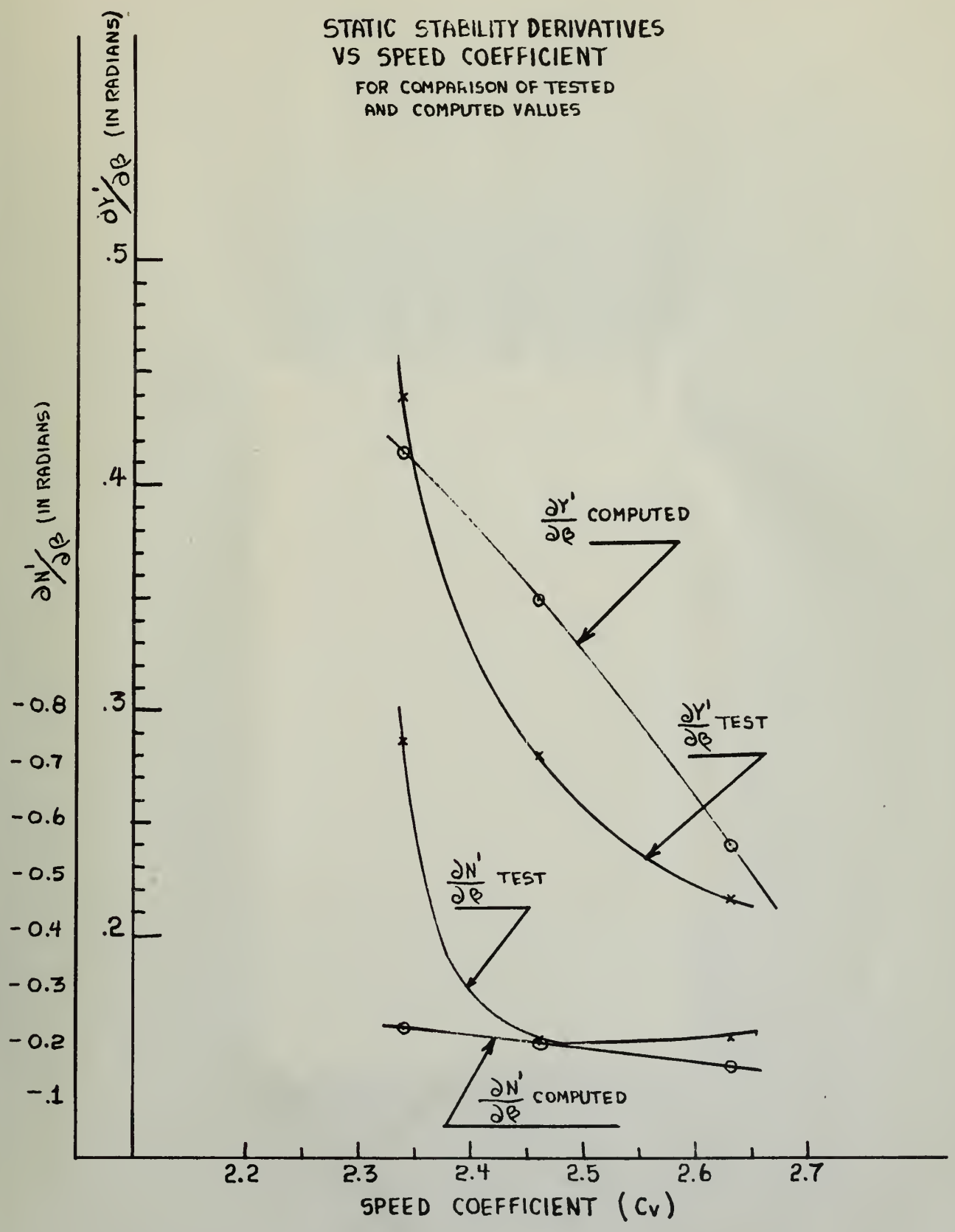
STATIC STABILITY DERIVATIVES
VS SPEED COEFFICIENT
FOR COMPARISON OF TESTED
AND COMPUTED VALUES
$\partial N'/\partial\beta$ (IN RADIANS)
$\partial Y'/\partial\beta$ (IN RADIANS)
-0.8
-0.7
-0.6
-0.5
-0.4
-0.3
-0.2
-.1
.5
.4
.3
.2
$\frac{\partial Y'}{\partial\beta}$ COMPUTED
$\frac{\partial Y'}{\partial\beta}$ TEST
$\frac{\partial N'}{\partial\beta}$ TEST
$\frac{\partial N'}{\partial\beta}$ COMPUTED
2.2
2.3
2.4
2.5
2.6
2.7
SPEED COEFFICIENT (Cv)

FIG. 22

Date Due

Thesis
D19 De Callies 17305
Evaluation of static stability derivatives from standards yawing tests.